FINAL REPORT

Development of a 100 kw L-band TWT for Phased Arrays

By

M. V. Purnell

Contract No. AF 19(628)-500

Subcontract No. 259

File No. W-J 64-434R24

13 March 1964

WATKINS-JOHNSON COMPANY
3333 Hillview Avenue
Palo Alto, California

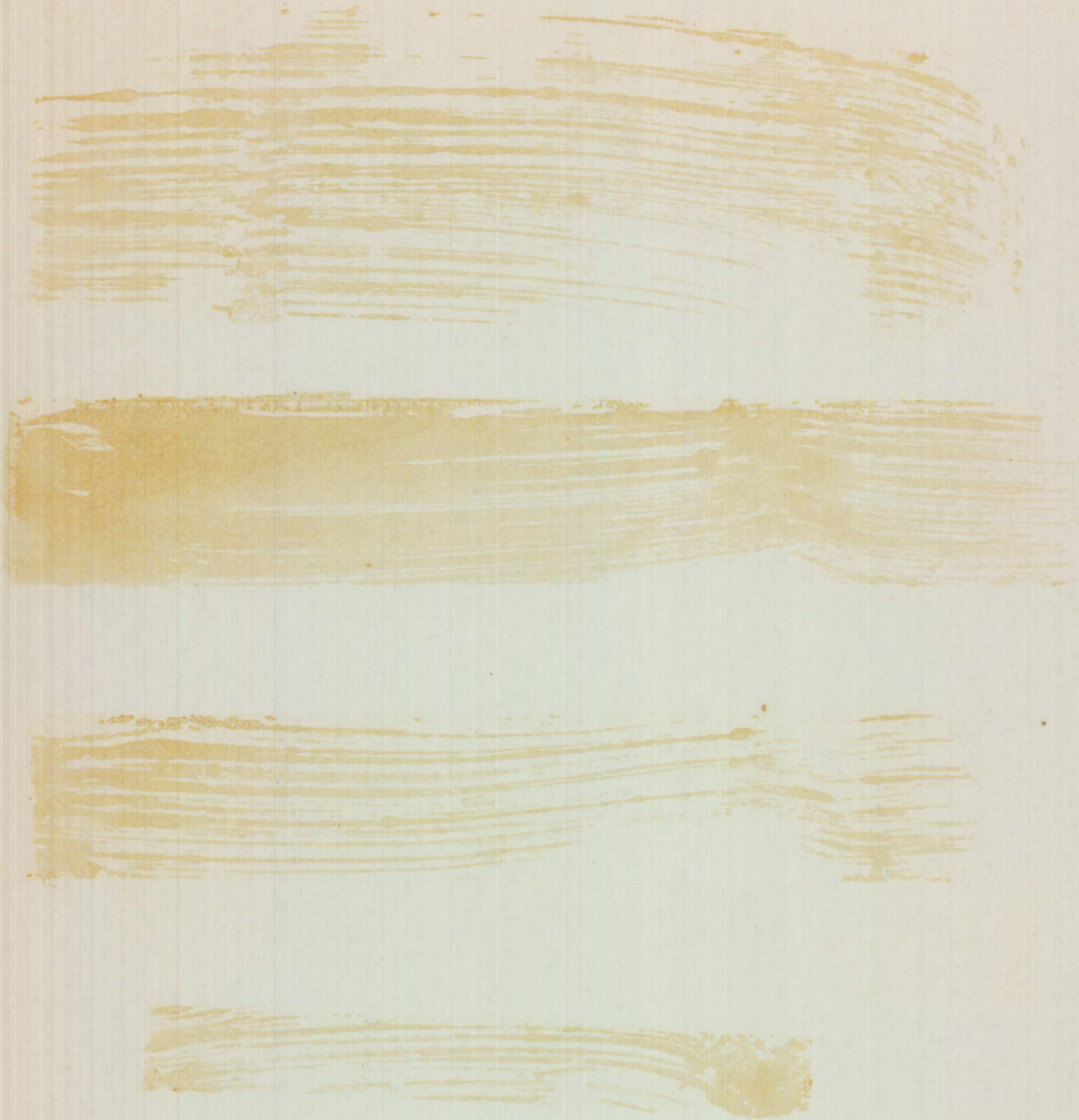

ABSTRACT

The purpose of this program is to develop a gridded 100 kilowatt L-band traveling-wave tube suitable for application in phased array radar systems.

A ring-bar circuit which operates at 23 kv was selected for use in this tube. A perveance 5 gridded solid electron beam gun was developed for this tube. The tube was focused using a solenoid, PPM and single reversal permanent magnet configurations. Power outputs in excess of 100 kilowatts were measured. Beam efficiencies in excess of 30 percent were also measured. Perveance 5 x 10^{-6} electron gun uses a copper mesh grid with a μ of 100.

The tube was constructed as a grounded cathode tube which required unique techniques for mounting the circuit, the anode, making connections to the circuit, and the development of an rf match to the circuit.

The work reported in this document was performed under subcontract to Lincoln Laboratory, a center for research operated by Massachusetts Institute of Technology with the support of the United States Air Force under Contract AF 19(628)-500.

TABLE OF CONTENTS

LIST OF ILLUSTRATIONS

LIST OF ILLUSTRATIONS (Continued)

LIST OF ILLUSTRATIONS (Continued)

LIST OF TABLES

INTRODUCTION

The purpose of this program is to develop a grounded cathode traveling-wave tube with a gridded gun for use in phased arrays. The tube is designed to have a hundred kilowatts peak power and 13 db of gain over the 1240 to 1340 Mc frequency band. The tube is to have a minimum phase sensitivity to changes in rf drive or changes in power supply voltages.

This tube utilizes a ring-bar interaction circuit and a perveance 5×10^{-6} gridded electron gun. The combination of the high interaction impedance of the circuit and the high perveance electron gun results in high gain per wavelength. The tube being electrically short has good phase stability relative to variations of power supply voltages.

This tube is unique in that the cathode is operated at ground potential and the collector and circuit are operated with positive potentials. To construct this grounded cathode tube it was necessary to isolate the anode and the interaction circuit from ground. It was necessary to build an input coaxial matched to the tube which would capacitively couple to the circuit, stand off the 23 kv of circuit voltage and provide a good rf match. To connect the circuit to the high voltage without removing appreciable rf power a coaxial high voltage lead was constructed in the collector to connect high voltage from the circuit. This coaxial lead in the collector contains a high pass filter which has approximately an attenuation of 40 db to the rf in the frequency band.

Five devices were constructed, two of which were grounded cathode tubes, one grounded circuit beam tester, one grounded circuit tube, and one grounded cathode beam tester. The grounded circuit beam tester was constructed to evaluate the focusing of the gridded perveance 5 electron gun. The grounded circuit tube was built so that the electrical design of the tube could be evaluated without solving all the mechanical problems associated with the grounded cathode tube. The grounded cathode beam tester was used for focusing tests of the beam with the magnetic geometry the same as in the case of the grounded cathode tube.

This report describes the electrical design of the tube and the predicted phase stability of the tube; The construction of each of the devices and the tests results obtained from these devices. A conclusion and summary is included at the end of the report.

DESIGN OF THE TUBE

General Consideration

The electrical tube design is based on 100 kw of output power, a saturated gain of 13 db over a frequency band of 100 Mc centered at 1.29 Gc. The tube was designed to be short electrically so that small changes in power supply voltages cause small changes in the phase of the output. To make the tube electrically short a perveance 5×10^{-6} solid electron beam was selected for use in the tube. The electron gun has high μ grid which allows the tube to operate at very high prf with little modulation power required to charge tube capacitances as compared with a cathode modulated tube.

A ring bar or counterwound helix was selected as the circuit to be used in the tube because it gives a very high impedance and more than adequate bandwidth. The circuit is inexpensive to construct and is made by sawing slots into a piece of tubing from alternate sides. At 1270 Mc the structure is large enough so that it can be easily brazed to ceramic wedges which will conduct the heat to the outside of the tube.

Electrical Design Calculation

The output power is a minimum of 100 kw over the frequency band 1.24 Gc to 1.34 Gc. The minimum beam efficiency based on the circuit voltage, beam current and output rf power, is assumed to be 25 percent, then:

$$\text{Beam power} = \frac{\text{RF power}}{\text{beam efficiency}} = 400 \text{ kw}$$

$$\text{The circuit} \quad V_o = \left(\frac{\text{Beam Power}}{\text{Perveance}}\right)^{0.4} = \left(\frac{P_B}{IP}\right)^{0.4}$$

$$V_o = \left(\frac{400,000}{5 \times 10^{-6}}\right)^{0.4} = 23 \text{ kv}$$

$$I_o \text{ (Beam)} = V_o^{3/2} \, IP$$

$$I_o = \left(2.3 \times 10^4\right)^{3/2} \, 5 \times 10^{-6}$$

$$I_o = 17.4 \text{ Ampere}$$

The voltage on the axis of the beam is less than the circuit voltage V_o by ΔV where

$$\frac{\Delta V}{V_o} = f\left(P, \frac{a}{b}\right) \qquad \frac{a}{b} = 1.38$$

P = perveance of the gun

a/b = ratio of circuit ID to beam O.D.

$\frac{\Delta V}{V_o}$ can be determined from Fig. 1.

$$\frac{\Delta V}{V_o} \approx 1 - (1 - 2K)^{1/2} \quad \text{where } K = .122$$

$$\frac{\Delta V}{V_o} = .13$$

$$V_{axis} = V_o - \Delta V = V_o(1 - .13) = 20 \text{ kv}$$

$$\frac{u_o}{c} = .266 \quad \text{where } u_o = \text{electron velocity on the axis of the beam}$$

For this design $\frac{v}{c} = \frac{u_o/c}{1 + Cb} = .229$

so the $\gamma a_i = \frac{2a_i \pi f}{v} = 1.24$ for v/c of .229 and $2a_i = .830$ inches

where $2a_i$ = inside diameter of the ring-bar circuit
f = 1.29 Gc at the mid-band of the tube

2b the beam diameter was selected as 0.6 inches.

Cold test measurements were made on the ring-bar circuit to determine the following:

the ω-β diagram as shown in Fig. 2
the phase velocity vs frequency as shown in Fig. 3
the interaction impedance vs frequency as shown in Fig. 4
(the data, in Figs. 2 to 4, was taken for a ring-bar circuit geometry as shown in Fig. 5)

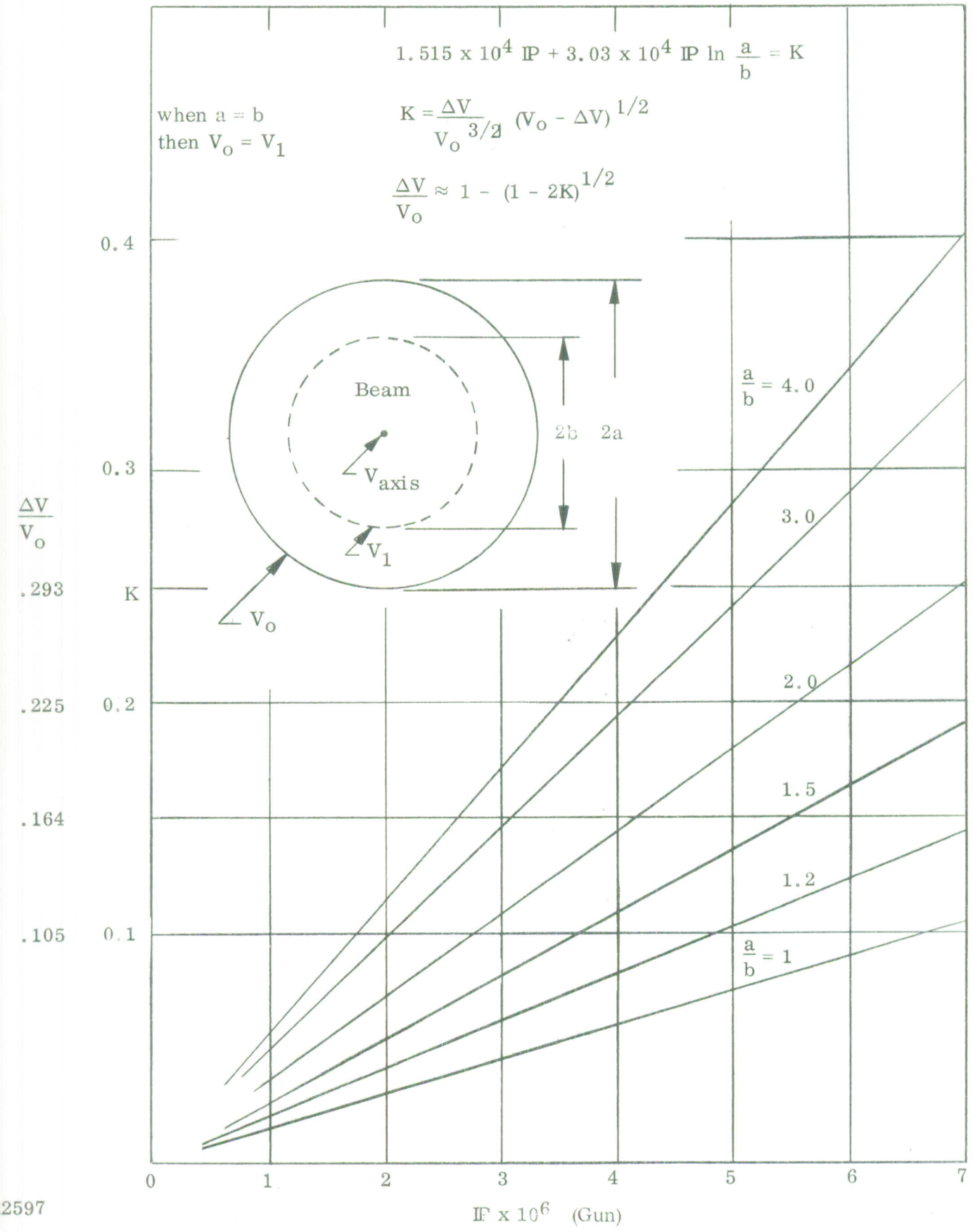

Fig. 1 - This graph is used to determine the value of $\Delta V/V_o$ which is the potential difference between the circuit potential and the potential on the axis of the beam.

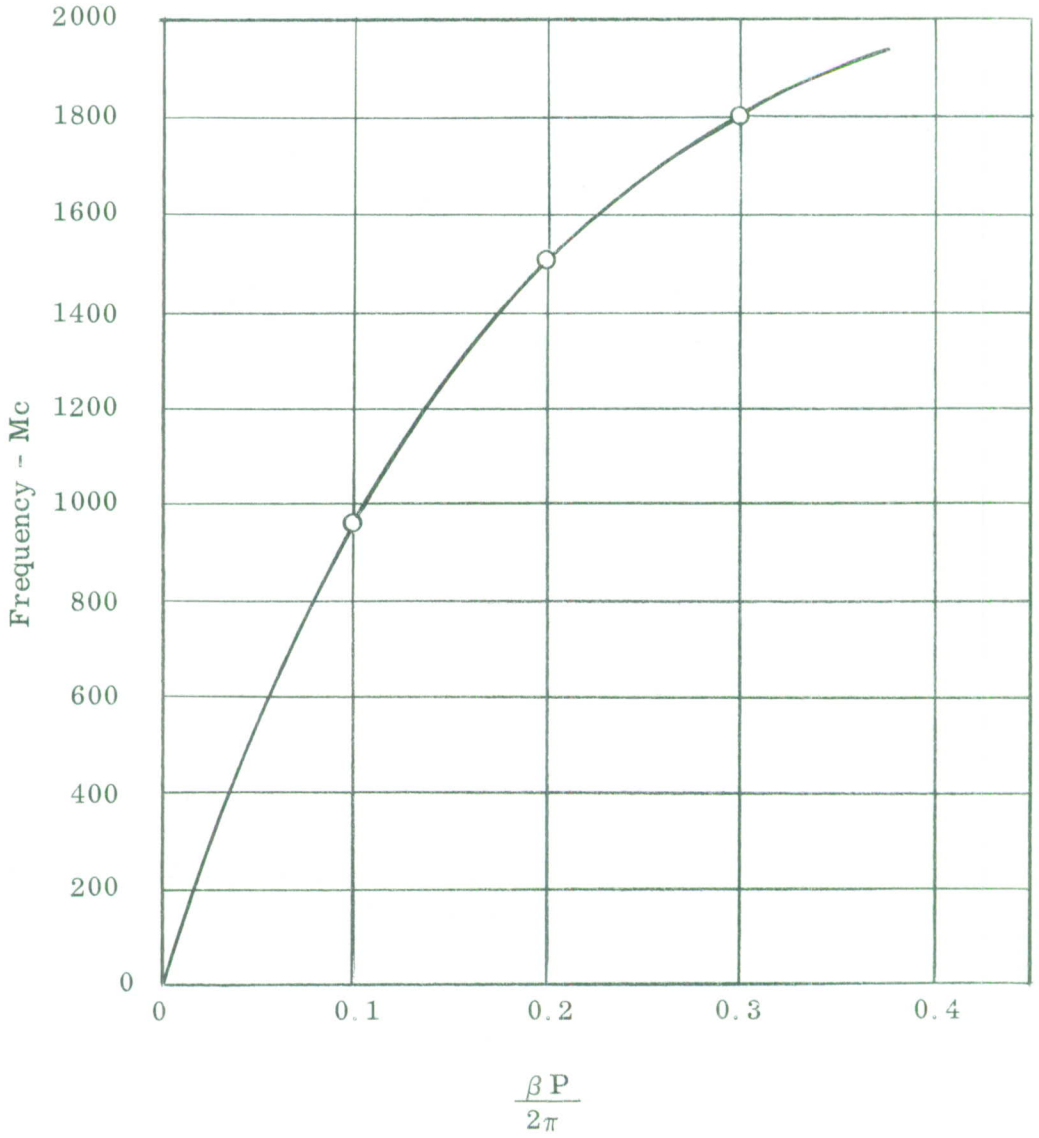

Fig. 2 - ω-β diagram of the ring-bar circuit used in the 100 kw L-band TWT. The geometry of the circuit and its support is shown in Figure 5.

12591

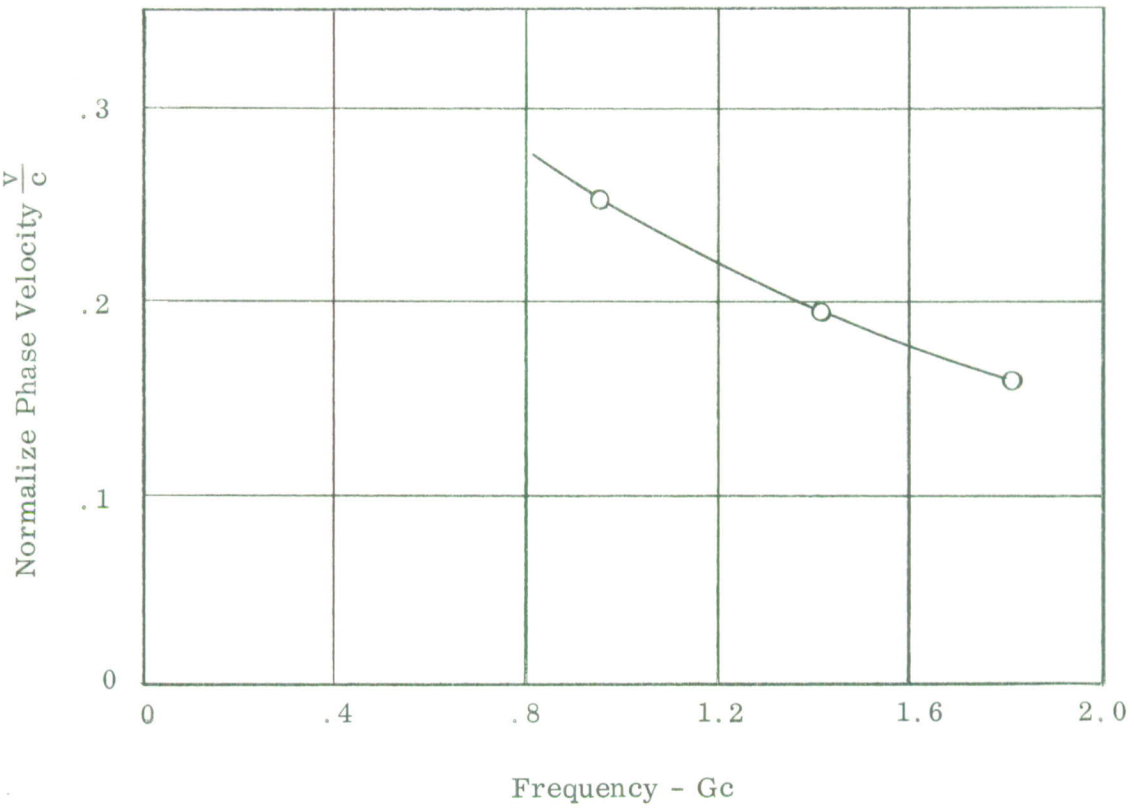

Fig. 3 - Phase velocity vs. frequency for the ring-bar circuit with the geometry as shown in Figure 5.

12592

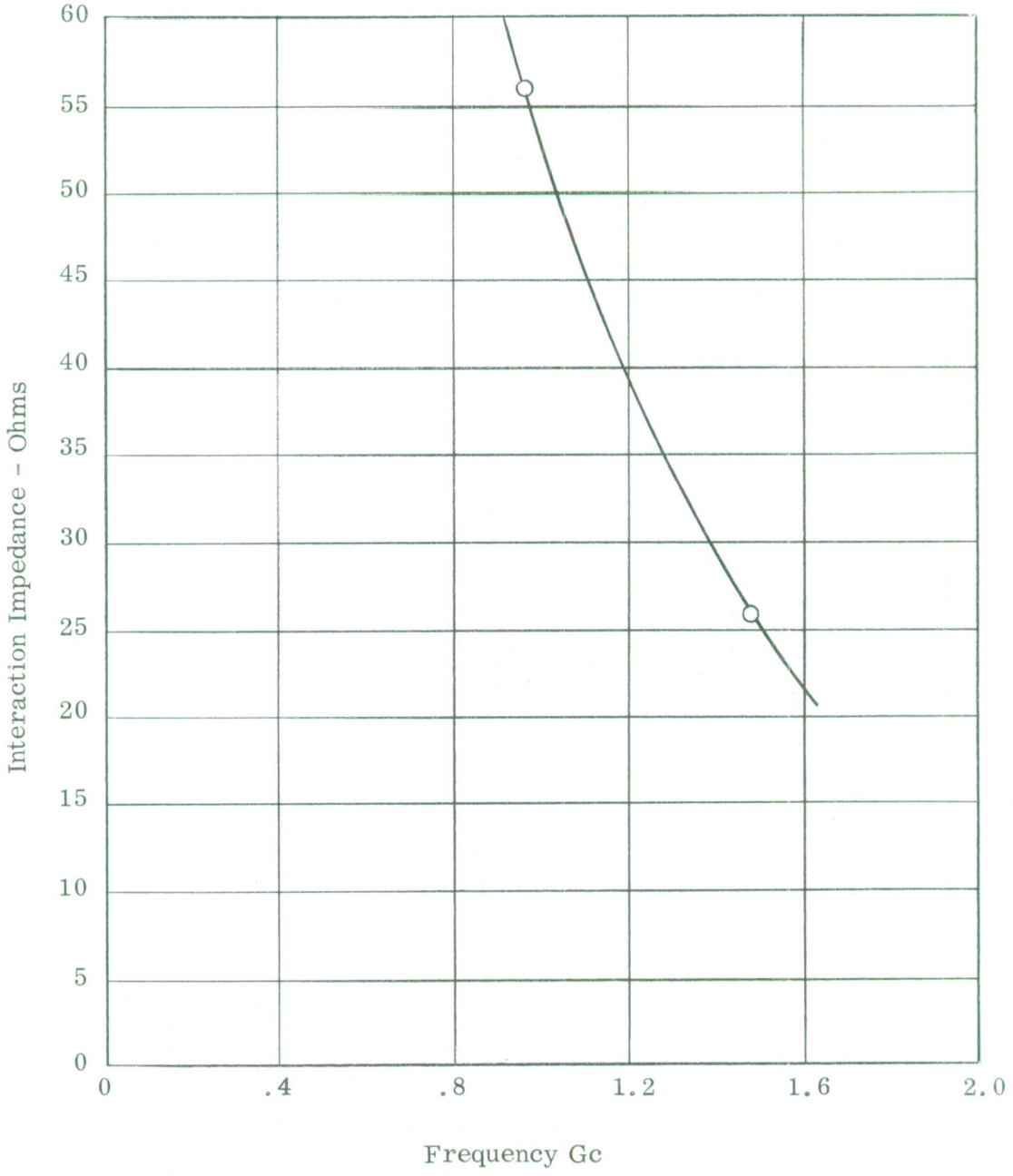

Fig. 4 - Interaction impedance vs frequency of the ring-bar circuit used in the 100 kw L-band TWT. See Fig. 5 for geometry of circuit.

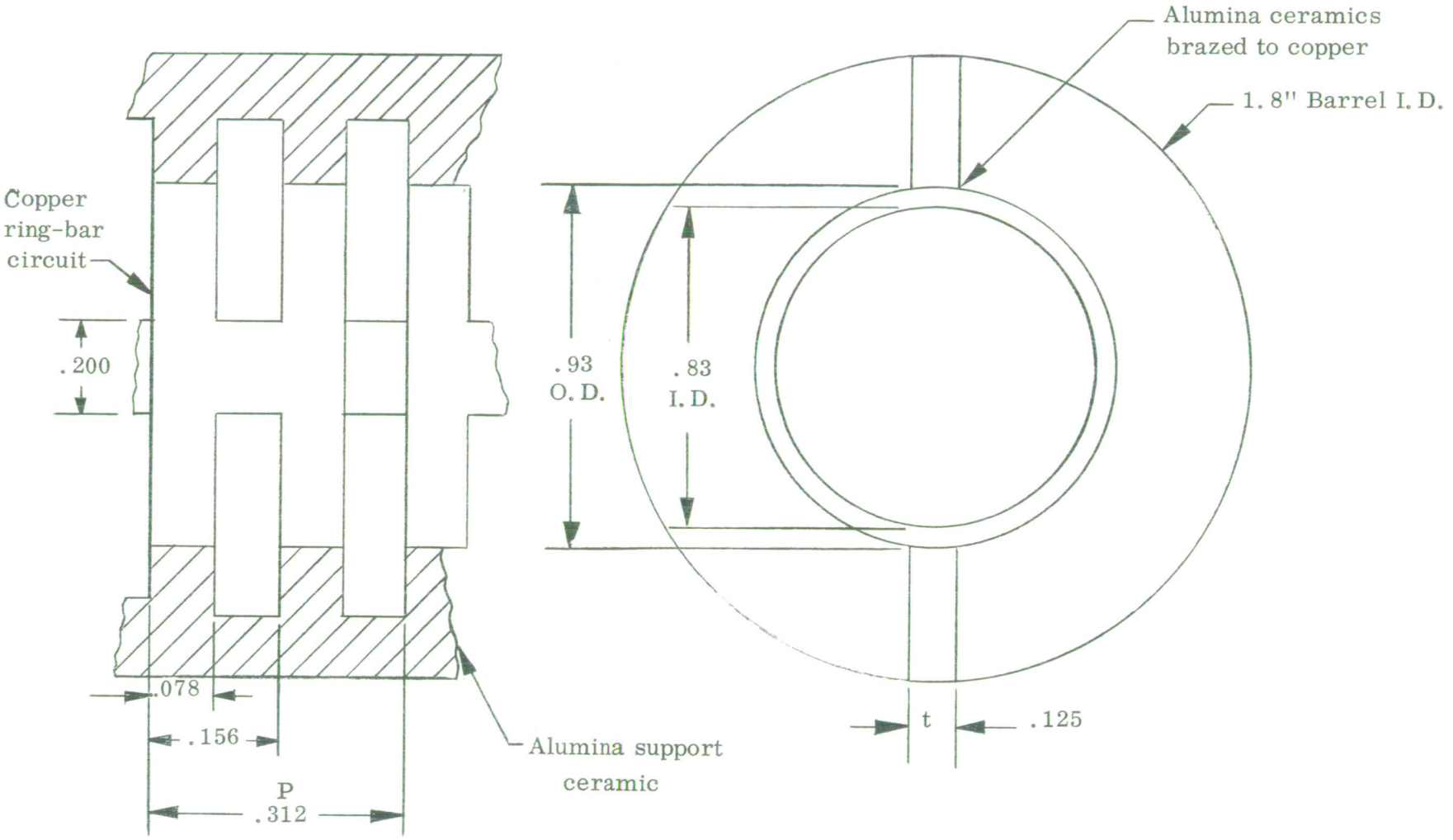

Fig. 5 - Geometry of ring-bar circuit, supporting ceramics and barrel used to determine cold test values shown in Figs. 2 to 4.

The pierce gain parameter can be calculated based on the measured value of interaction impedance K at 1.29 Gc.

$$K = 34 \text{ ohms}$$

$$C^3 = \frac{K I_o}{4 V_{axis}} \qquad C = .196 \text{ at } 1.29 \text{ Gc}$$

To find QC one must determine the value of $\frac{\omega_q}{\omega}$.

The plasma wavelength λ_p can be found as follows:

$$\lambda_p = \frac{1.25 \left[V_{axis} \text{ (KV)} \right]^{3/4} 2b\text{(cm)}}{I_o^{1/2}} = \lambda_p \text{ inches}$$

$$\lambda_p = 4.32 \text{ inches}$$

$$\omega_p = 74.2 \times 10^9 \frac{u_o/c}{\lambda_p \text{ (inches)}} = 4.6 \times 10^9$$

$$\frac{\omega_p}{\omega} = \frac{\omega_p}{2\pi f} = \frac{4.6 \times 10^9}{2\pi (1.29) \times 10^9} = .57$$

The plasma frequency reduction factor R can be found in Branch and Mehran[1] to be 0.42 for $\frac{a}{b} = 1.38$ and $\gamma b = \frac{\gamma a_i}{a/b} = 0.9$

$$\frac{\omega_q}{\omega} = R \frac{\omega_p}{\omega} = 0.42 \times 0.57 = .239$$

$$QC = \frac{1}{4 C^2} \left[\frac{\omega_q/\omega}{1 + \omega_q/\omega} \right]^2$$

$$QC = .242$$

The loss parameter d is based on a measure value of 1/4 db per guide wavelength of the ring-bar circuit. This value can be found as follows:

$$d = \frac{.01836\ L}{C} \qquad \text{where L is loss in db per guide wavelength}$$

$$d = \frac{(.01836)\ (.25)}{.196} = .0236$$

The maximum value of $\frac{X_1}{1 + bC}$ can be found from curves in the Birdsall and Brewer[2] paper.

$\frac{X_1}{1 + bC}$ is a function of C, QC, and d

$$\frac{X_1}{1 + bC} = 0.7$$

$$BC = 54.6\ \frac{X_1\ C}{1 + Cb} = 7.5 \text{ db per guide wavelength of the circuit}$$

The initial loss factor A can also be found from the paper by Birdsall and Brewer to be:

A = -7 db for QC = .242 and C = .196

The total electronic gain required to obtain 13 db of saturated gain is BCN. N = number of guide wavelengths along the ring-bar circuit. BCN = 13 db + 6 db for saturation + 7 db for initial loss

$$BCN = 26 \text{ db}$$

$$N = \frac{BCN}{BC} = \frac{26}{7.5} = 3.47 \text{ wavelengths}$$

$$\lambda g = \frac{(v/c)\ c}{f} = \frac{(.229)\ 30 \times 10^9}{1.29}$$

$$\lambda g = 5.35 \text{ CM}$$

$$\lambda g = 2.1 \text{ inches}$$

The length of the circuit will then be

$$L = \lambda g\ N = (2.1)\ (3.47) = 7.29 \text{ inches}$$

The design values of the tube at mid-band as calculated using the measured value of interaction impedance are listed in Table I.

TABLE I

Summary of Tube Design Data at 1.29 Gc

Circuit Perveance (V_o = 23 kv)	5×10^{-6}
Beam Perveance (V_{axis} = 20 kv)	6.5×10^{-6}
Circuit efficiency	25%
Beam efficiency	29%
Beam current I_o	17.5 amps
u_o/c	.266
v/c at 1.29 Gc	.229
γa_i at 1.29 Gc	1.24
$2a_i$ (circuit ID)	.830 inches
2b (beam diameter)	.600 inches
K at 1.29 Gc	34 ohms
C at 1.29 Gc	.196
ω_q/ω	.239
QC	.242
λ_p	4.32 inches
d	.0236
b	.816
y_1	-1.1
$\frac{X_1}{1 + Cb}$	0.7
gain	13 db saturation
BC (db/λg)	7.5
A	-7 db
BCN	26 db
N	3.47 λg
λg at 1.29 Gc	2.1 inches
L = N λg	7.29 inches

Phase Sensitivity of the Design

The phase stability of the tube is determined by the stability of the cathode to circuit voltage and the cathode to grid voltage. The total phase length of the tube will change during saturation of the tube. This results from the reduction in the average velocity of the electron in the beam. Changes in the magnetic field also vary the phase of the tube. Changes in magnetic field will be small. The effect of changing circuit voltage, grid voltage and varying the input drive on phase can be predicted on the basis of work by Bean and Blattner[3].

The change in phase caused by a 1 percent change in cathode to circuit voltage can be found as follows:

$$\frac{\Delta \phi}{\Delta V_o/V_o} = 180 \left[(1 + bC)(0.42 + 0.07\,QC) + cy - 1 \right] \text{ X N degrees}$$

$$\frac{\Delta \phi}{\Delta V_o/V_o} = (180) \left[(1.16) \left[0.42 + (0.07)(.242) \right] - .216 - 1 \right] 3.47$$

$$= 180\ (.609)\ (3.47)$$

$$\frac{\Delta \phi}{\Delta V_o/V_o} = -380 \text{ degrees}$$

For a 1 percent change in voltage

$$\Delta \phi = 3.8 \text{ degrees for a } \frac{\Delta V_o}{V_o} = .01$$

The change in phase caused by a 1 percent change in cathode to grid voltage can be found as follows:

V_g = voltage cathode to grid

$$\frac{\Delta \phi}{\Delta V_g/V_g} = 90\ C\ (1 + QC)\ N \text{ degrees}$$

$$= (90)\ (.196)\ (1.242)\ (3.47)$$

$$\frac{\Delta\phi}{\Delta V_g / V_g} = 76.1 \text{ degrees}$$

$$\Delta\phi = .761 \text{ degrees for 1 percent change in } V_g$$

The total change in phase caused by saturation power can be found as follows:

$$\Delta\phi_{total} = -\frac{13.7\, P_{rf}}{P_B} \times \frac{[1 + bC]\,[0.42 + 0.07\, QC] + cy - 1}{BC} \text{ radians}$$

$$\Delta\phi_{total} = -\frac{13.7\, P_{rf}}{P_B} \frac{-.609}{7.5} \text{ radians}$$

$$\Delta\phi_{total} = 1.11 \frac{P_{rf}}{P_B} \text{ radian} = 63.6 \frac{P_{rf}}{P_B} \text{ degrees}$$

Fig. 6 is a plot of rf power output vs input drive power. This data was obtained from measurements made on tube No. 1 which is a grounded circuit tube with 90 kw to 100 kw of output power over the band 12.4 Gc to 13.4 Gc. This data was used to plot phase shift vs input drive power (see Fig. 6). From this data the maximum phase change per db change in drive power can be found to be 1.75^{o}/db.

Table II is a summary of the results of the phase stability calculations. The corresponding value of phase stability of the specification is also listed.

The phase uniformity from tube to tube will be determined by the matches on the input, output, and the match of the internal attenuator. If for example, the match at the input and output had a VSWR of 2 to 1 at any phase and the attenuator had no reflection and infinite loss the phase would not vary, due to input and output load matches. If one is to limit the phase variation from tube to tube over the operating band to a maximum value of 4.5^{o} with VSWR's of 2 to 1 of any phase on the output and input loads then the attenuator must have at least α db of attenuation with no reflection.

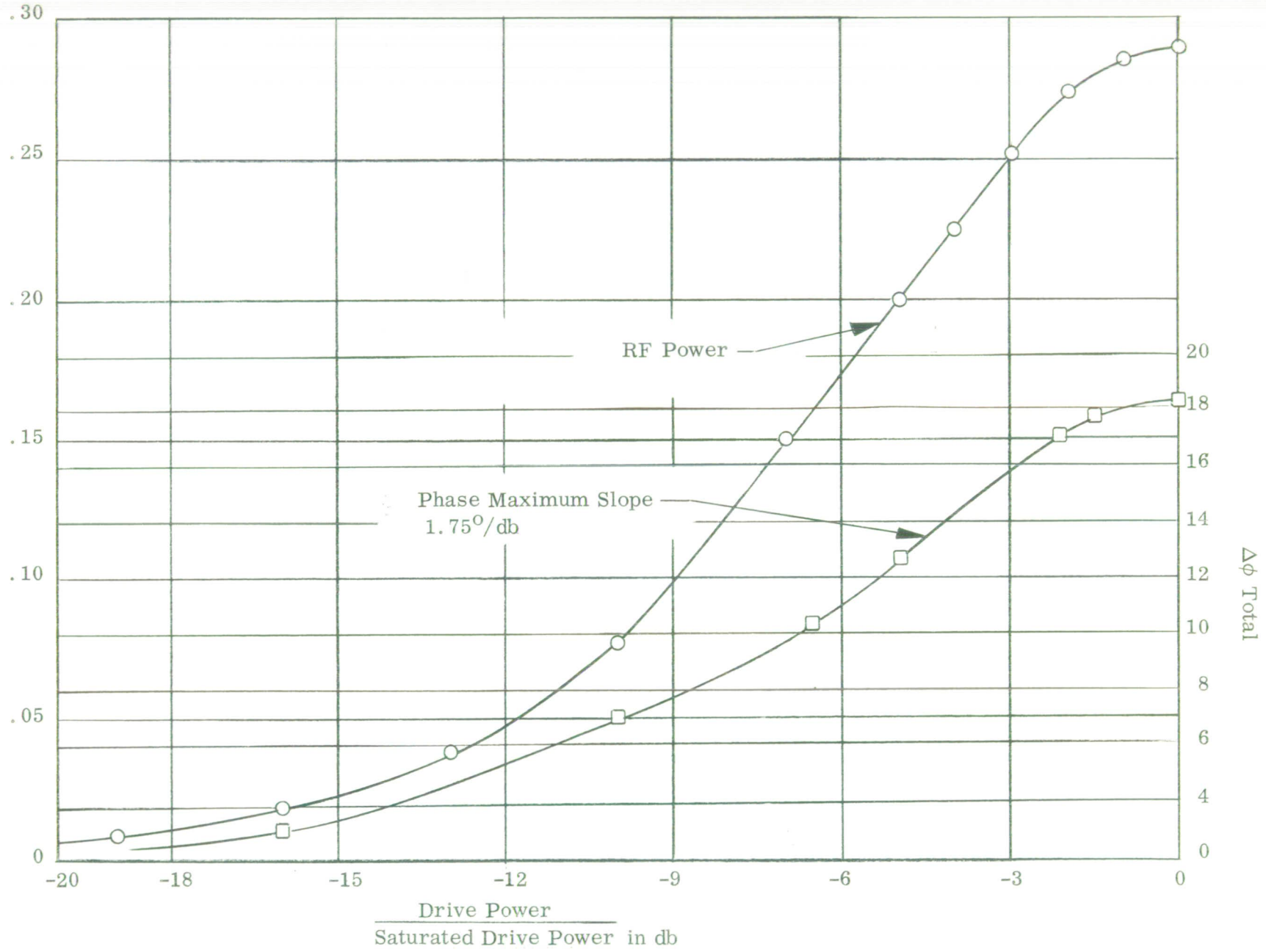

Fig. 6 - Measured data showing output power vs drive power on tube No. 1. This measured data was used to determine the total phase change vs drive power. From the total phase change the max change of phase for 1 db change in drive was found to be 1.75 degree/db.

TABLE II

Summary Of Phase Stability Calculations

Parameter Varied	Variable Parameter	Calculated $\Delta\phi$	Specification $\Delta\phi$
Cathode Circuit Voltage	$\frac{\Delta V_o}{V_o} = .01$	3.8^o	3.5^o max
Cathode Grid Voltage	$\frac{\Delta V_g}{V_g} = .01$	$.76^o$	3.5^o max
Input Power	Change of 1 db	1.75^o	2^o max

The value of α can be found as follows:

$$V_r = V_o \rho_1 \rho_2 G$$

$$\tan \phi \approx \phi = \frac{V_r}{V_o} = \frac{\rho_1 \rho_2 G}{\sqrt{\alpha}}$$

where $G = \sqrt{40}$ which corresponds to 16 db of power gain

$$\rho_1 = \frac{1}{3} \quad \rho_2 = \frac{1}{3} \text{ on a 2 to 1 VSWR}$$

$$\phi = \left(\frac{4.5}{2}\right)\left(\frac{\pi}{180}\right) = .0392 \text{ radians}$$

$$\sqrt{\alpha} = \frac{\rho_1 \rho_2 G}{\phi} = \frac{\sqrt{40}}{9\ (.0392)} = 17.9$$

$$\alpha = (17.9)^2$$

$$\alpha_{db} = 20 \log_{10} 17.9 = 20(1.25) = 25 \text{ db}$$

$$\alpha_{db} = 25 \text{ db}$$

The maximum attenuator reflection ρ_α than will cause ϕ to vary less than $\pm 2.25^o$ or a total of 4.5^o can be found as follows, if the gain between attenuator and the output is 13 db.

$$\phi = .0392 = \rho$$

$$\rho_\alpha = \frac{.0392}{\rho_1 G} = \frac{(0392)\,3}{20} = .0263$$

$$\rho_\alpha = .0263$$

on maximum attenuator VSWR $= \frac{1 + .0263}{1 - .0263}$ at the output end of the attenuator.
VSWR = 1.055

Heat Transfer of Circuit Assembly

To determine the beam transmission necessary for the tube to produce 1 kilowatt of average power a calculation of the hot spot temperature of the ring-bar circuit was made. In this calculation the ring-bar circuit was supported exactly as in the present tube except the supporting ceramics are of beryllia instead of the presently used alumina.

The geometry of the heat flow problem is shown in Figs. 7 and 8. As a starting point it is assumed that the outside edge of each of the supported ceramics is held at $T_1 = 40^{\circ}C$. The problem is then broken into three regions. Regions one and two are across the beryllia ceramic. Region one is from the edge of the ceramic to the tooth and region two is the ceramic tooth to the ring-bar circuit. Region three is the ring-bar circuit from the ceramic to hot spot on the ring. These three regions are shown in Figs. 8 and 9.

The temperature at the boundary between each region was calculated (see App. 1) starting with $T_1 = 40^{\circ}C$ at the edge of the ceramic for all power levels. Fig. 9 shows the temperature T_1 through T_4 vs power dissipation per ring of the circuit. At 60 watts per ring the hot spot temperature on the circuit is $369^{\circ}C$. This temperature should not degrade the tube performance. Satisfactory performance may be obtained at even higher temperatures.

The specific heat conductivity of beryllia is not constant, but is a function of temperature, this is plotted in Fig. 10. The temperature drop across beryllia is not proportional to power. This is shown on the temperature vs power per ring curves in Figs. 8 and 9.

The transmission of the tube must be greater than some value that would cause 60 watts to be dissipated on any one ring of the circuit. There are two sources of power to the ring. The first is the beam power and the second is the rf power absorbed due to the slight loss of the circuit.

The ring-bar circuit of the tube has a 1 db or less loss over approximately 8 inches. There are approximately 50 rings on an 8 inch circuit. At the output end of the tube power dissipation per ring due to rf power is approximately 5 watts per ring. Calculation of rf power dissipation is contained in Appendix 1.

The second source of power dissipation on the ring-bar circuit is due to beam interception. It is assumed that 95 percent transmission can be obtained with no drive (93 percent is the present obtainable value). It would be expected that this 5 percent

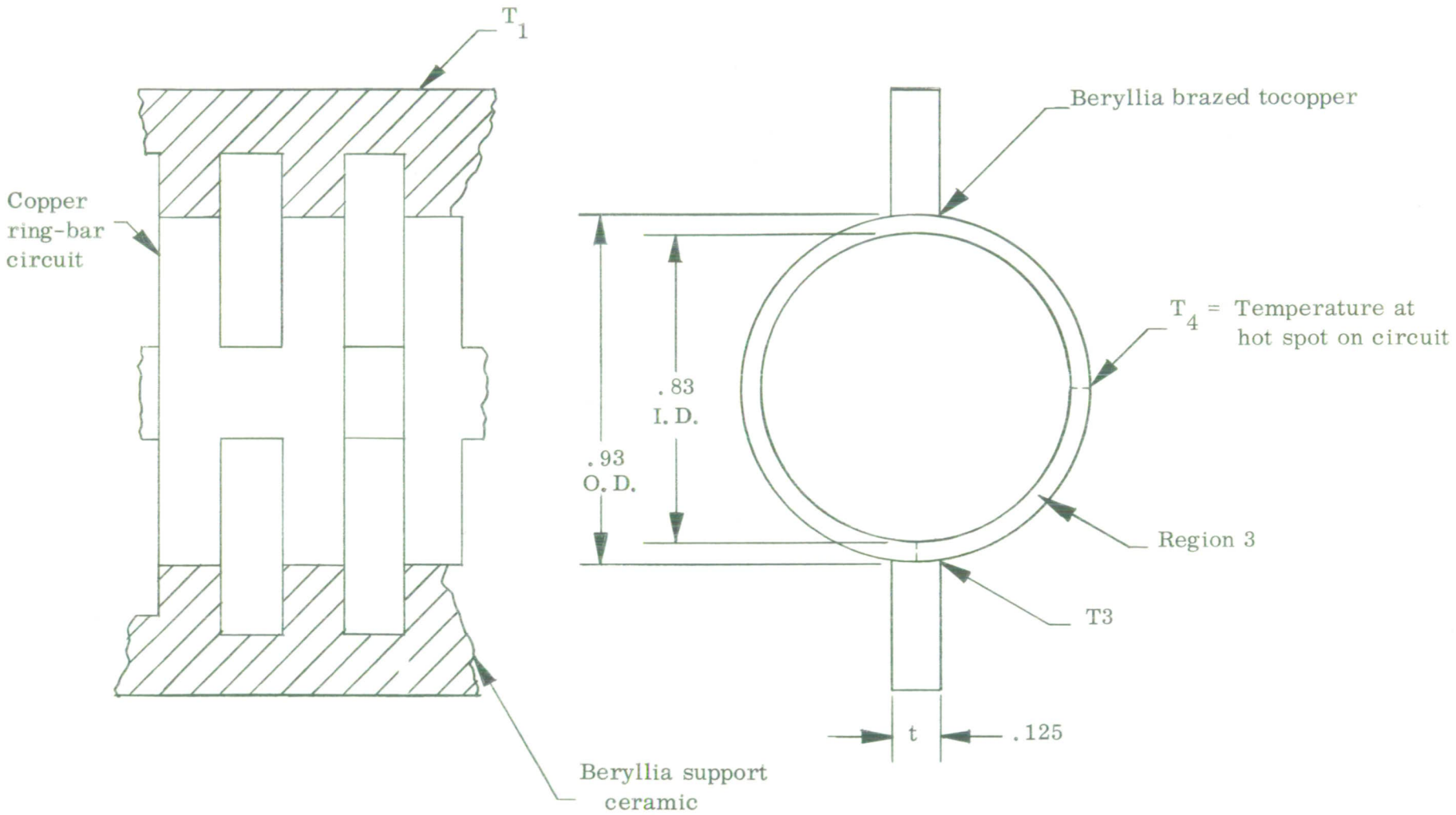

Fig. 7 - Geometry of ring-bar circuit and supporting ceramics.

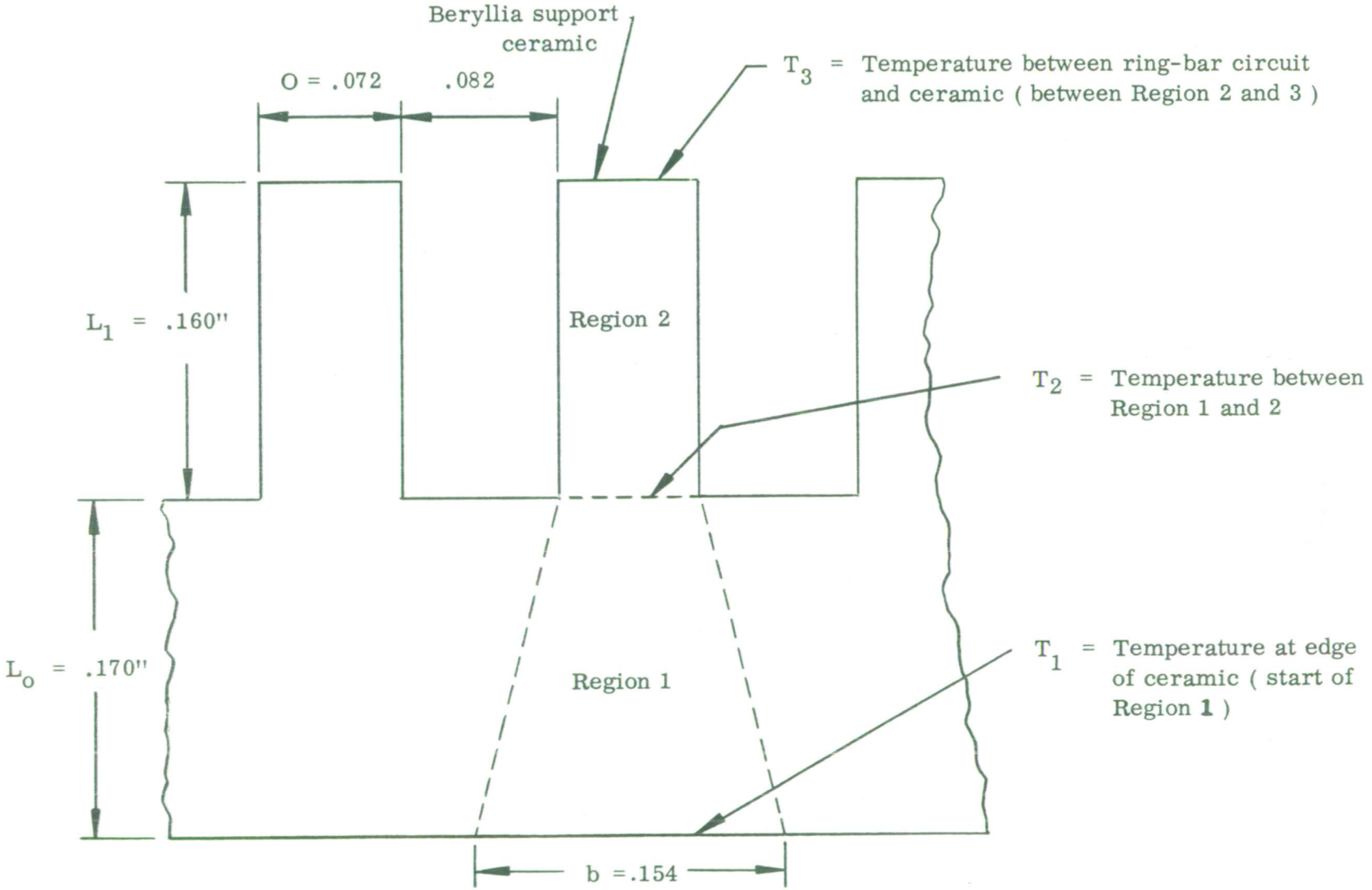

Fig. 8 - Details of regions 1 and 2 of supporting ceramic for the ring-bar circuit.

The geometry shown in Fig. 1 shows the location of T_1 thru T_4.

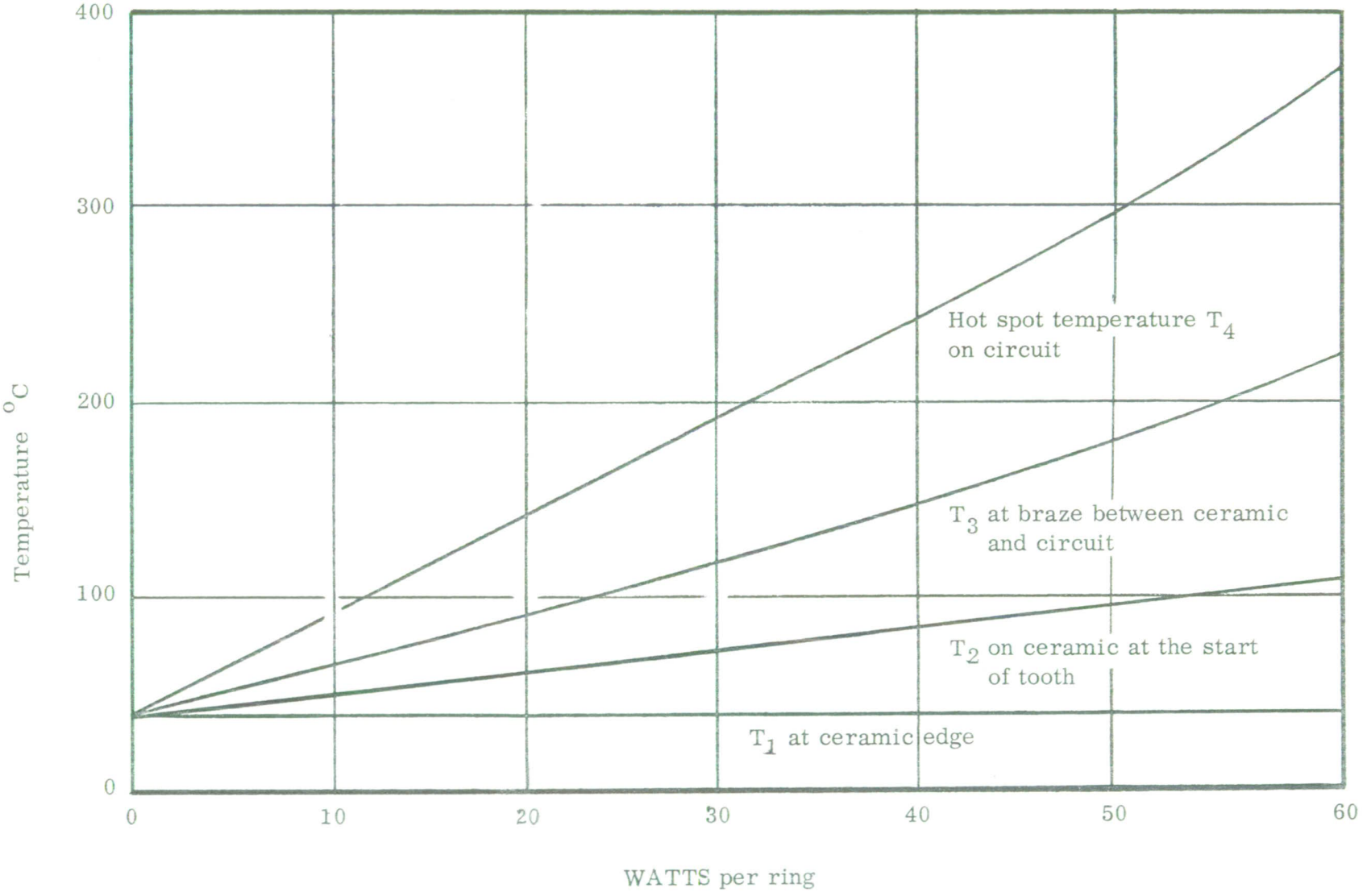

Fig. 9 - Temperature T_1 through T_4 vs average power dissipation per ring. These curves are for two (2) ceramics per circuit. This data can be used to determine the temperatures using three (3) ceramics per circuit.

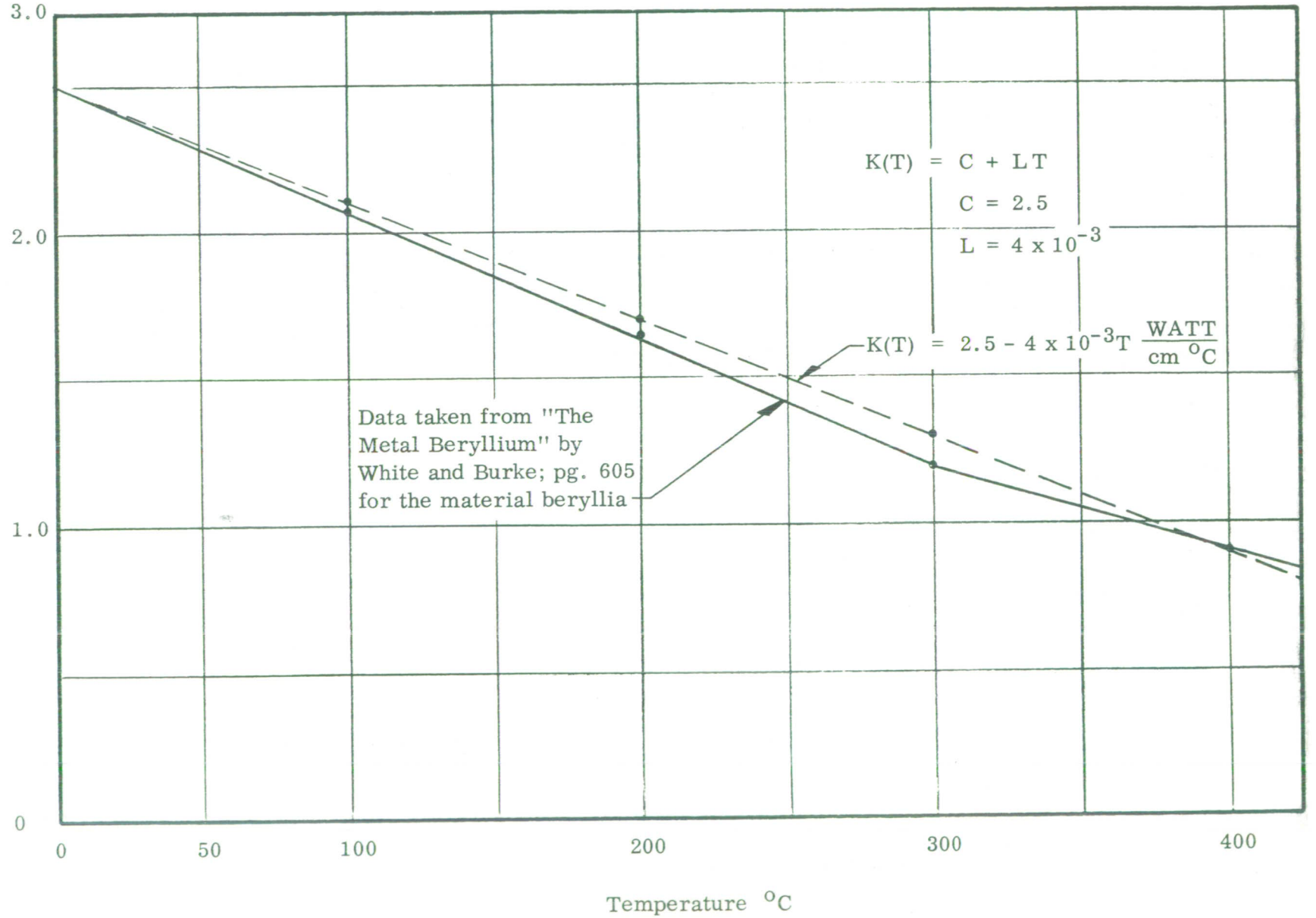

Fig. 10 - Specific heat conductivity of beryllia vs temperature.

beam interception would occur near the start of the circuit or after the magnetic-field reversal. Under saturated rf drive, rf defocusing will occur. It would be expected that beam interception on the circuit would occur near the output due to rf defocusing. It is assumed that all rf defocusing occurs over the last inch of the ring-bar circuit. (The circuit has about 3 db gain per inch.)

It is also assumed that the 5 percent beam interception without drive is distributed equally over the circuit rather than early in the circuit and after the reversal. On this basis the tube should operate with 85 percent transmission and 1 kilowatt average power as shown in Appendix 1.

In the calculations it was assumed that two support ceramics were used to conduct the heat from the ring-bar circuit. If three (3) support ceramics were used instead of two (2) a lower hot spot temperature on the circuit will result, or transmission may be less for the same hot spot temperature. Using Fig. 9 one can estimate these effects. Using three (3) ceramics at 60 watts per ring the operating point of the ceramics shift to 40 watts/ring on the curve. This corresponds to $T_4 = 250^{\circ}C$ on the curve. The correct temperature will be lower because the heat path in the copper ring is less than before by 2/3. Using the curve one can get the exact value as follows:

$$\left[T_4 - T_3\right] \frac{2}{3} + T_3 = \text{hot spot temperature}$$

$$[250 - 155] \frac{2}{3} + 155 = 219^{\circ}C$$

The hot spot temperature can be reduced from $369^{\circ}C$ to $219^{\circ}C$ by the use of three support ceramics instead of two. If three (3) ceramic supports are used and the average power per ring is 90 watts using Fig. 3, the hot spot temperature can be determined. The operating point of the ceramics corresponds to 60 watts/ring on the curve T_3 (60 watts/ring) = 223. The hot spot temperature T_4 can be found as follows:

$$T_4 = T_3 \left(\frac{60\ w}{ring}\right) + \left[T_4\ (60\ w/r) - T_3 \left(\frac{60\ w}{ring}\right)\right] \frac{2}{3}$$

$$T_4 = 223 + [369 - 223] \frac{2}{3}$$

$$T_4 = 321^{\circ}C$$

The transmission at 90 watts per ring would be as follows using the same assumption as Appendix I.

RF loss	=	5.07 watts/ring
No drive interception	=	3.24 watts/ring
RF defocusing	=	81.69 watts/ring
Interception due to rf	=	$\frac{(81.69)(6.4)}{3300} = \frac{\text{(power per ring)} \frac{\text{rings}}{\text{inch}}}{\text{total beam power}}$
	=	15.8 percent
Total interception	=	15.8 + 5 = 20.8 percent
Transmission	=	79.2 percent at a hot spot temperature of 321°C using three (3) ceramic supports

Summary of results for 1000 watts of average power.

Power per Ring	Number of Ceramic Supports	Hot Spot Temperature	Transmission
60	2	369°C	85 percent
60	3	219°C	85 percent
90	3	321°C	79.2 percent

TUBE CONSTRUCTION AND TESTING

A total of five beam tests and tubes were built on the program. The first device to be constructed was a grounded circuit beam tester. The beam tester was constructed to evaluate the perveance 5×10^{-6} gridded gun. The beam test was built rather than a tube because it is much simpler to construct and test. Often a beam test will provide better focusing data than can be obtained from a tube because oscillations are not a problem.

The first tube to be constructed was a grounded circuit tube. Because the grounded circuit tube is much simpler than the grounded cathode tube information on the rf characteristics of the tube could be obtained much earlier in the program.

A grounded cathode beam tester and two grounded cathode tubes were constructed and tested on the program.

The construction and testing of the tubes is discussed in the following sections of the report.

Grounded Cathode Tube and Beam Tester

Beam Tester

Fig. 11 is a photograph of the beam tester. Fig. 12 shows the electromagnet used to supply a uniform field to the beam tester. The beam test was conducted in this electromagnet.

At a beam voltage of 15 kv and a total beam current of 9.25 amperes, 98.4 percent transmission to the collector was achieved with a magnetic field of 465 gauss. This magnetic field would scale to 575 gauss at 23 kv and 17.4 amperes beam current, a value that can be produced with a permanent magnet. The positive grid voltage swing required to produce a beam perveance of 5×10^{-6} is 1 percent of the beam voltage. That is, at a beam voltage of 23 kv, the positive grid swing would be 230 volts. The grid current at 15 kv is 2.2 amperes or 19 percent of the total cathode current. At 23 kv the grid current will be 4.1 amperes. At a beam voltage of 18 kv, the bias voltage could be reduced to just 53 volts before a 10 microampere change in tube current could be observed. The size

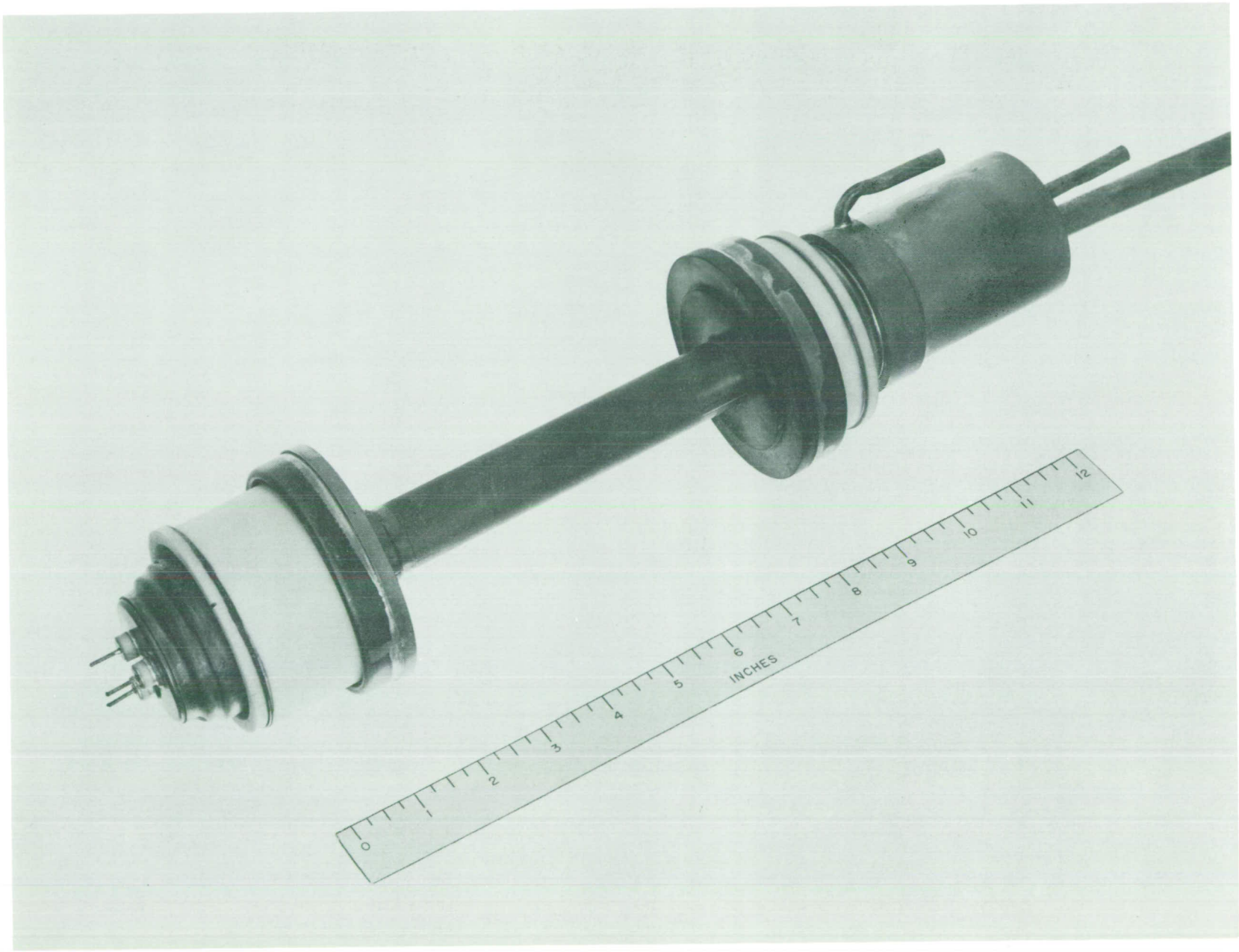

Fig. 11 - The beam tester tube used to measure the focusing characteristics of the perveance 5×10^{-6} gridded gun.

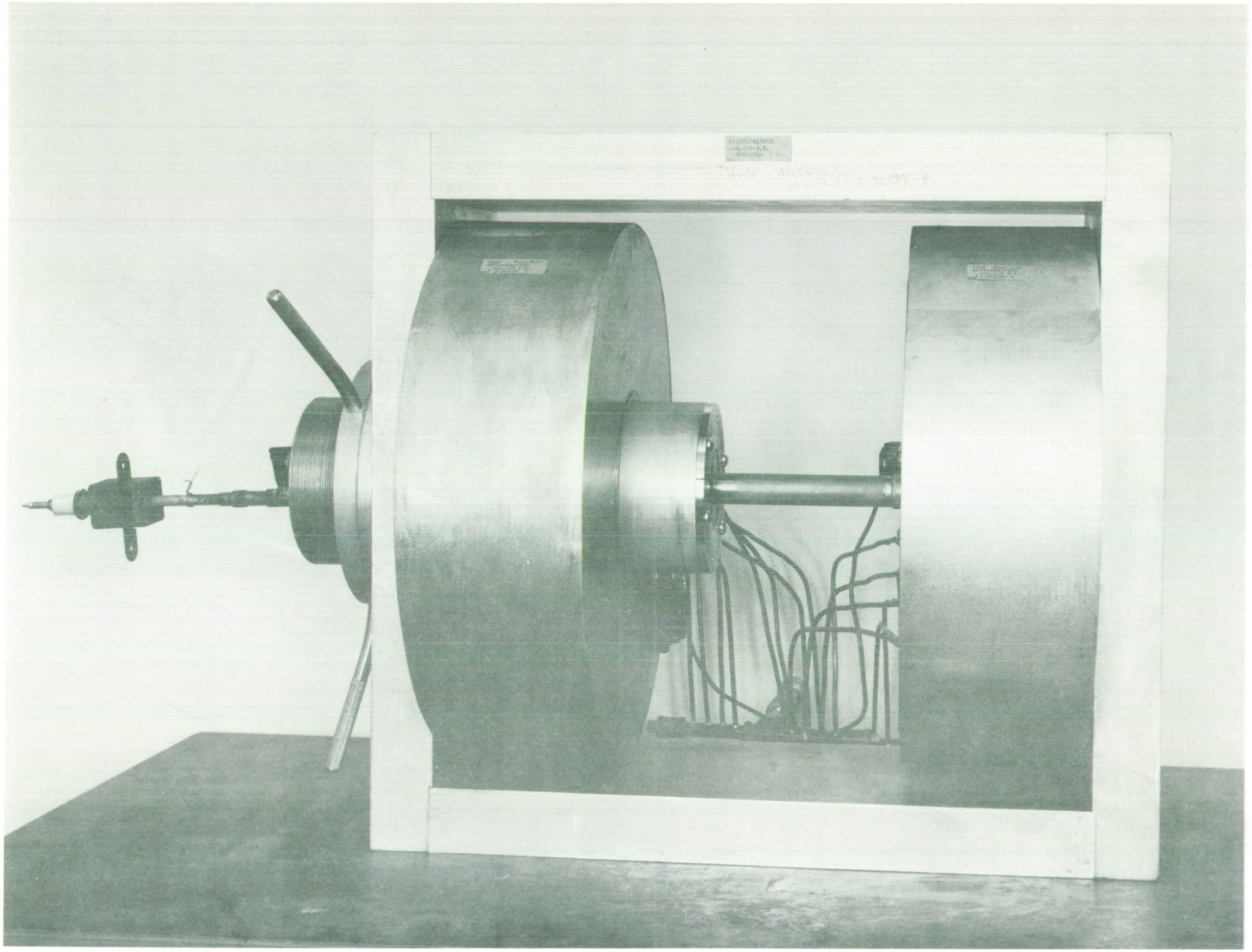

Fig. 12 - The electromagnet used to supply the magnetic field for focusing the beam tester tube.

of the holes in the grid can be increased considerably without increasing the required bias voltage to a prohibitively large value. The intercepted grid current would thus be reduced. The tube was not tested at 21 kv because of some arcing problems at about 18 kv.

The general conclusion that can be drawn from the above results is that the gridded gun works very well.

Grounded Circuit Tube

Construction of Tube No. 1

Fig. 13 is a photograph of the ring-bar circuit and ceramic wedges. The circuit assembly is extended part way out of the circuit cam. Some difficulty was encountered during the brazing of the ceramic wedges to the circuit. This was caused by the copper circuit expanding more than the ceramic wedges. It was necessary to key the ceramic wedges to the copper circuit during the brazing operation.

Fig. 14 is a photograph of a window assembly and the exploded view of the individual window parts. This window has a VSWR of 1.05 to 1 over the frequency band of the tube. Fig. 15 is a photograph of the rf window assembly and the adapter to LC connector and a section of RG-17/U coaxial line.

An exploded view of the gridded gun assembly is shown in Fig. 16. This gridded gun assembly was tested in the first grounded circuit beam tester.

The collector used on the grounded circuit beam tester and tube is shown in Fig. 17.

Small Signal Tests on Tube No. 1

The first experimental tube was a grounded circuit tube shown in Fig. 18. Initial testing could only be carried out at small signal level and at reduced beam current because the rf driver and the grid modulator had not been received. Small signal gain measurements were made at beam voltages of 21, 23, and 25 kv and at beam currents of 11 to 12 amperes. The design values were 23 kv and 17.4 amperes. The small signal gain as a function of frequency is shown in Fig. 19. The large gain variations at the higher

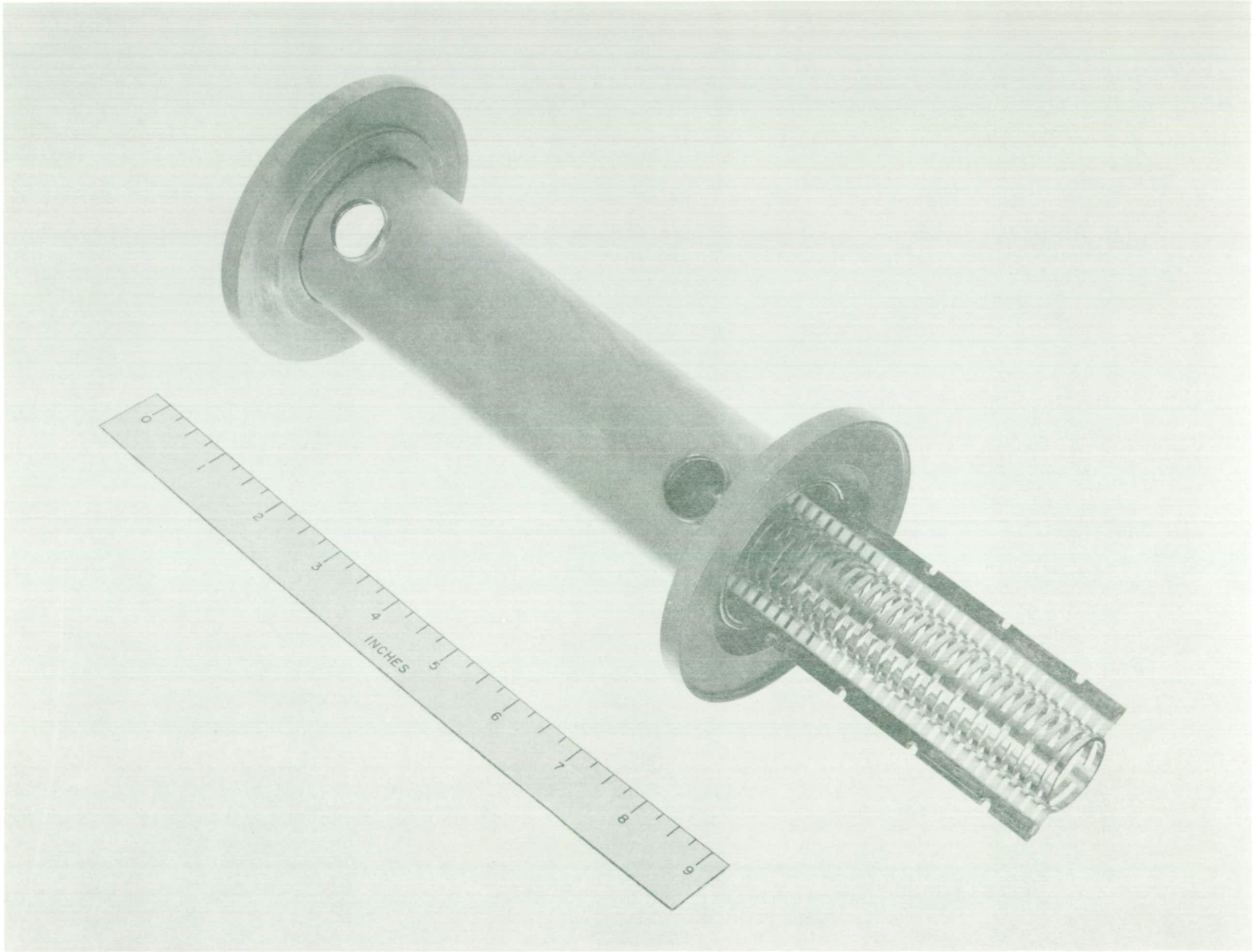

Fig. 13 – A copper ring-bar circuit brazed to notched ceramic slabs. The assembly is slipped into the circuit can and the slabs brazed to the can. Tube number 1 uses a similar circuit assembly.

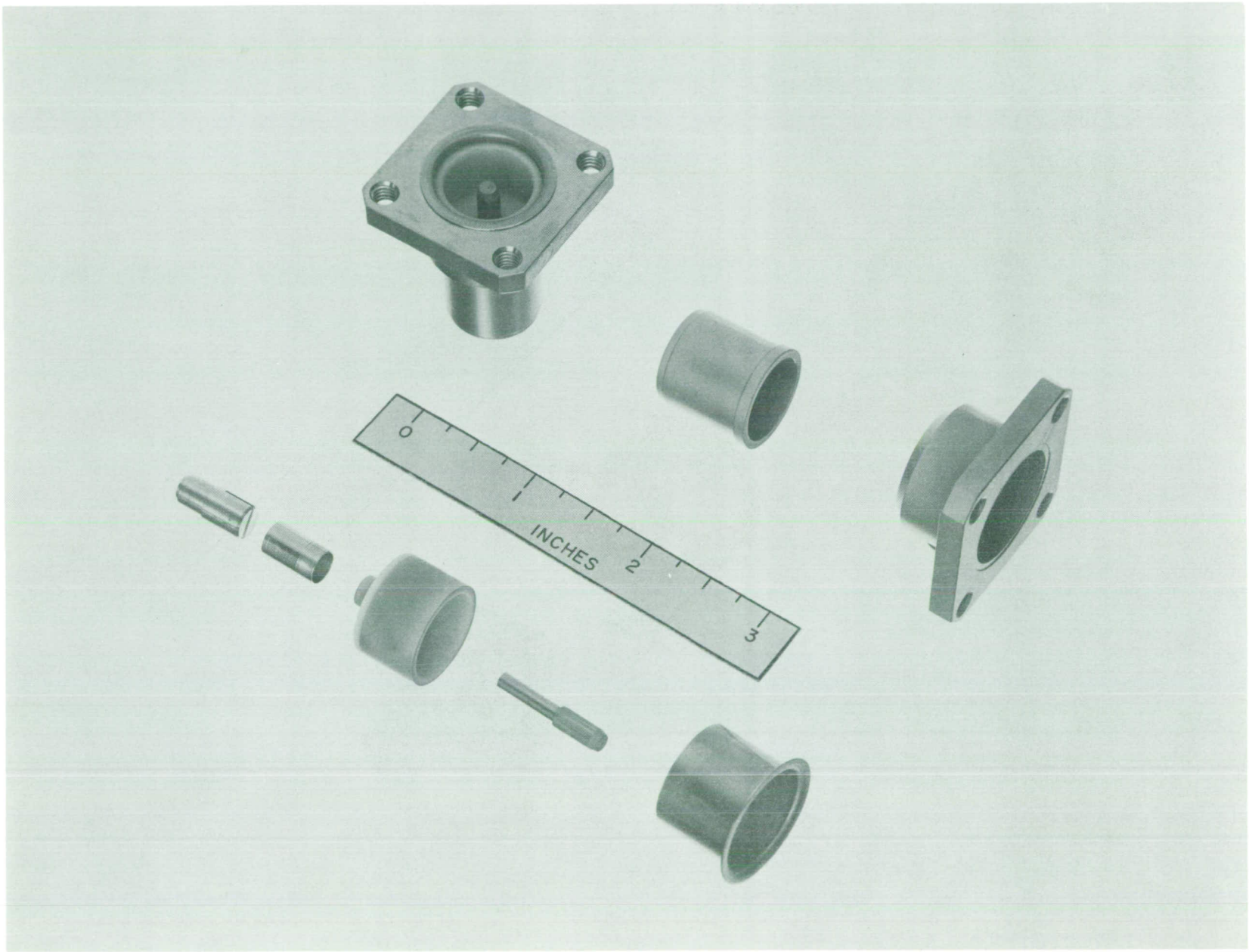

Fig. 14 - A complete rf window assembly and an exploded view of the component parts. This window was used in the grounded circuit tube.

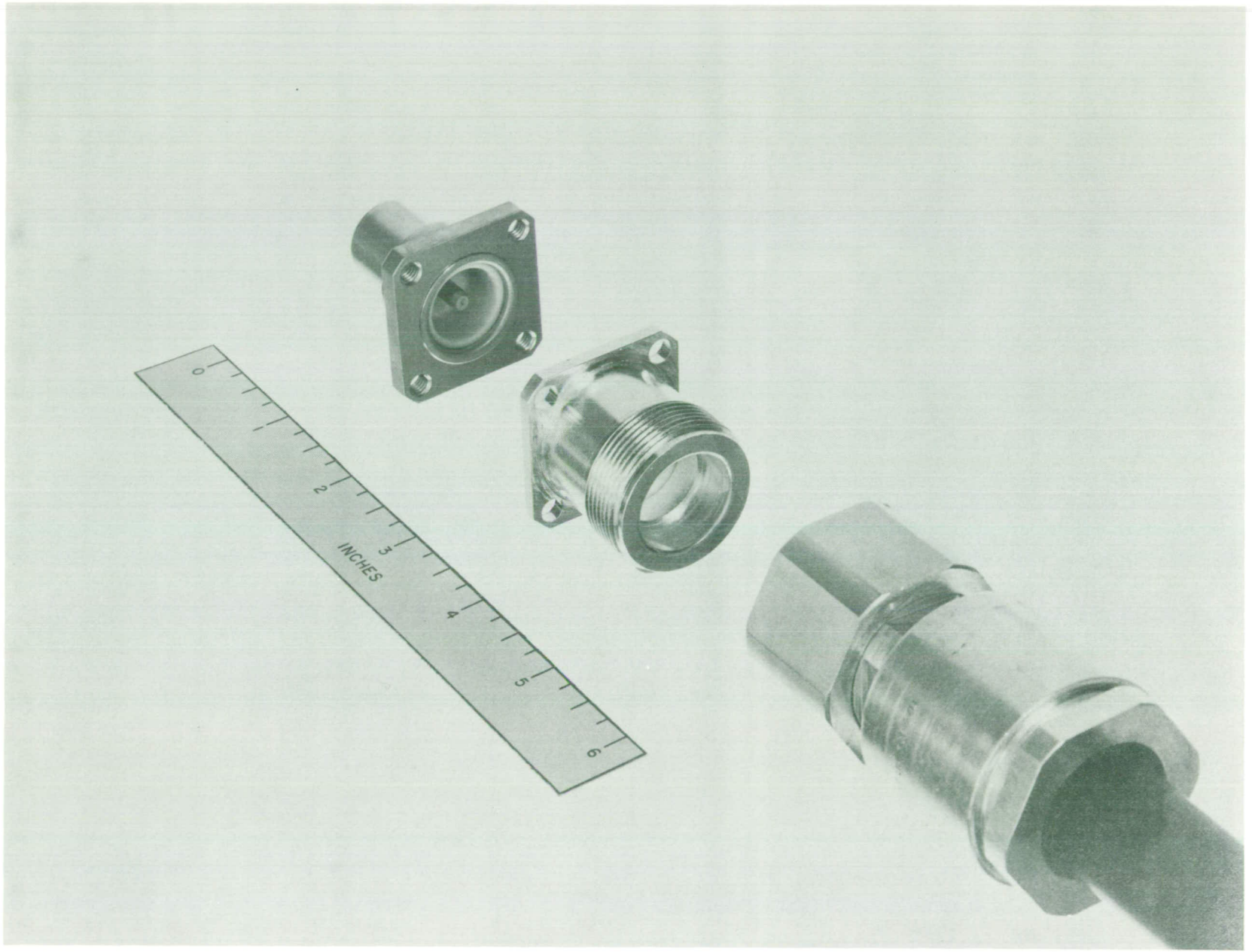

Fig. 15 - RF window assembly, adapter to LC connector and a section of RG-17/U coaxial line.

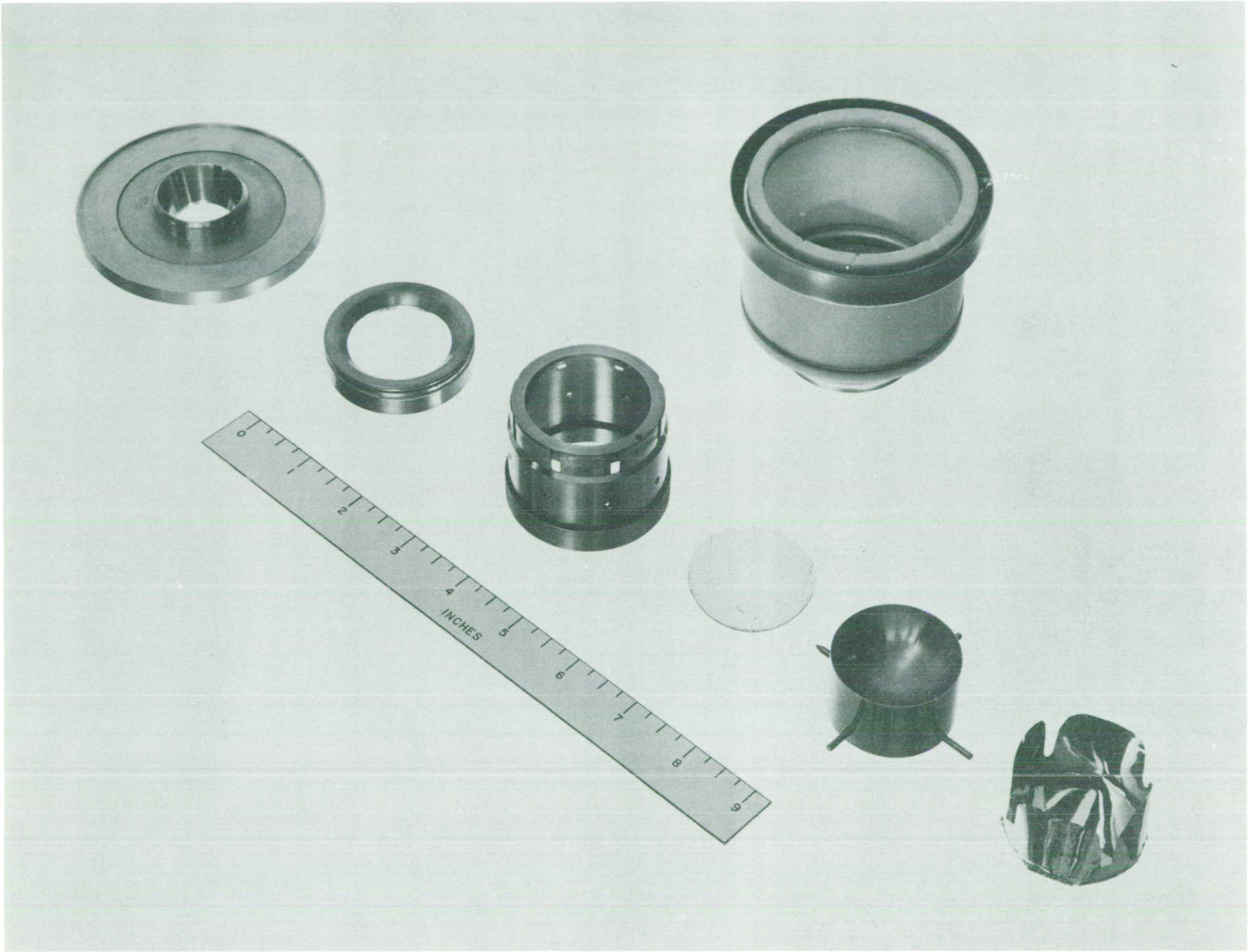

Fig. 16 - Exploded view of the gridded gun. At the upper left is the anode. Diagonally down to the right are the focus electrode, the grid support cylinder, the grid, the cathode, and a heat shield. At the upper right is the ceramic insulator assembly.

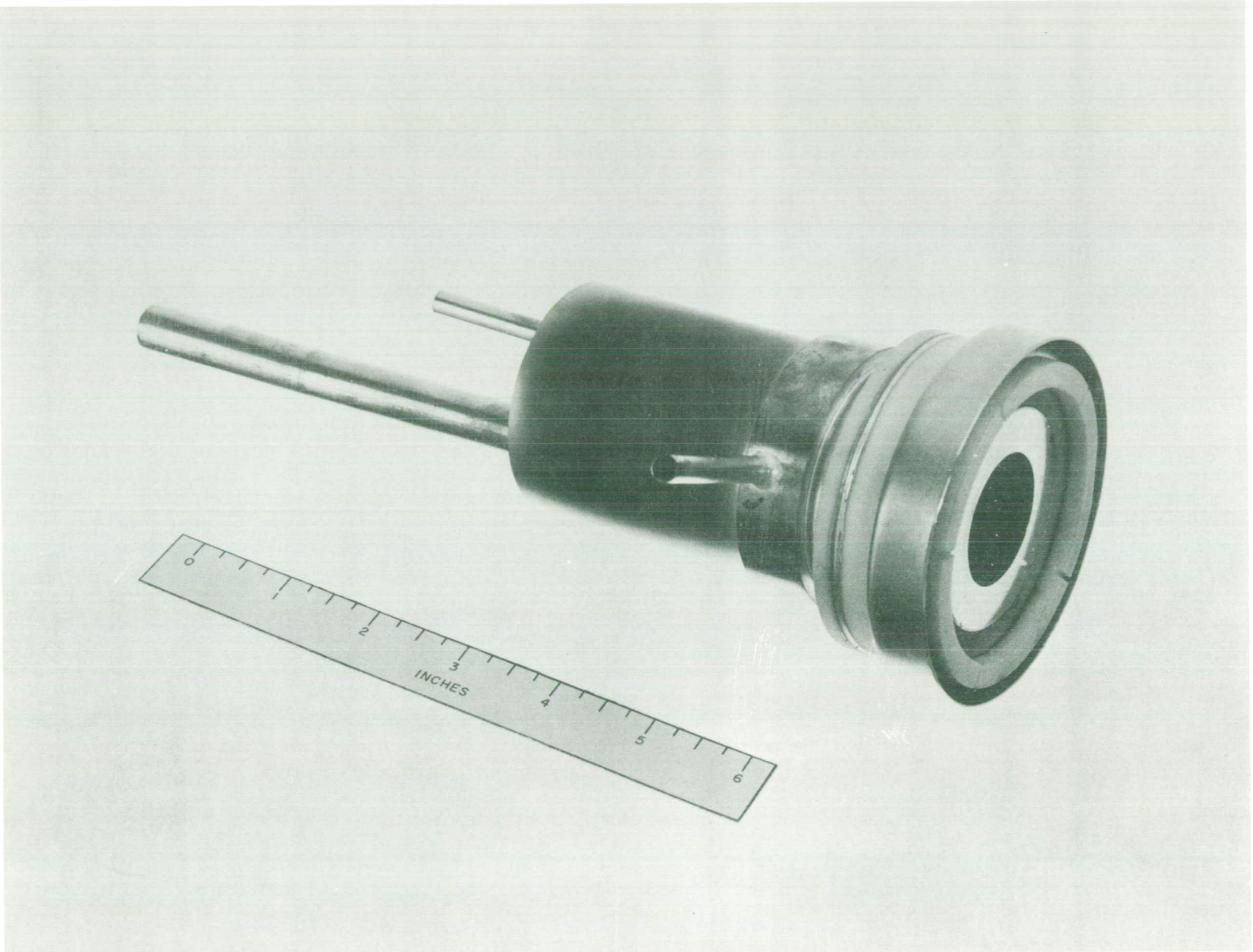

Fig. 17 - A collector assembly for the L-band amplifier.

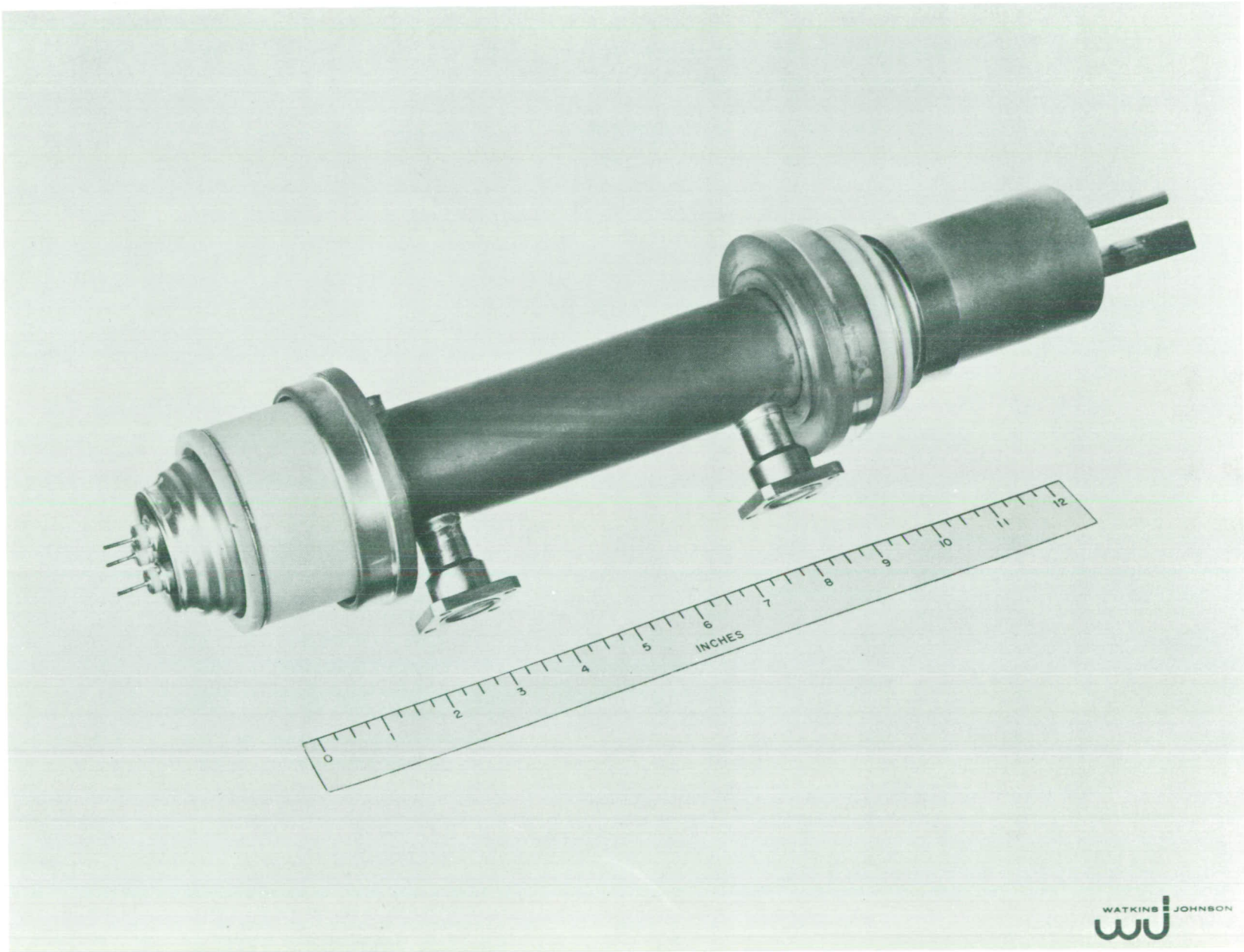

Fig. 18 - The first tube constructed was the grounded circuit tube shown above. Beam efficiency of over 30 percent was measured on this tube.

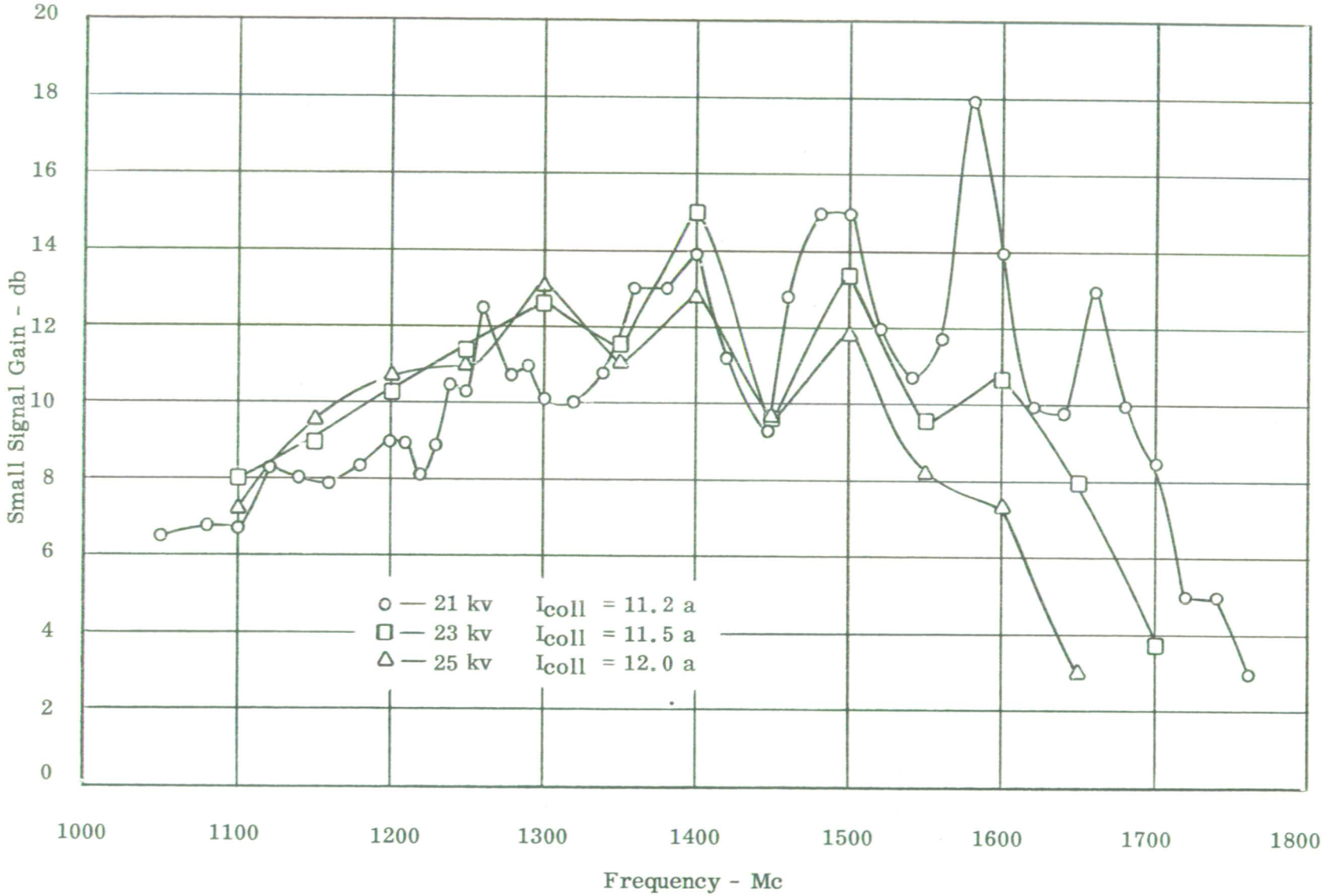

Fig. 19 - Measured small signal gain of experimental tube No. 1. The tube was tested at reduced current because a suitable grid modulator was not available. The gain is a little low and the best operating voltage is a little high. The peaks in the gain curves are due to a poor match.

frequencies are due to a bad match. The circuit assembly was not accurate and greater than 70 percent reflection coefficient was measured at some points in the band.

The tube actually operates best at 1300 Mc when the beam voltage is in the range 23-25 kv. The circuit will have to be made longer because the small signal gain is a little low even allowing for the reduced tube current. The tube was very stable at this reduced value of gain and tube current. The tube was quite free from arcing. Only two arcs occurred during a period of five hours of testing. No information could be obtained regarding efficiency because it was not possible to drive the tube to saturation. The tube was retested when the grid modulator is received.

Large Signal Tests on Tube No. 1

Experimental tube No. 1 was tested at large signal levels under various conditions of applied voltage, beam current, and magnetic field. Fig. 20 shows saturation curves when the dc voltage is 23 kv, the total beam current is 13.5 amperes, and the magnetic field is about 550 gauss. The beam efficiencies range from 28.7 percent to 32 percent in the frequency range 1250-1350 Mc. The saturated power output varies less than 0.5 db across that frequency range. The gain at saturation is about 10 db.

Fig. 21 is a plot of power output as a function of drive power for a dc voltage of 25.5 kv and a beam current of 14 amperes. The magnetic field in this case was about 685 gauss. Somewhat more gain and power output would have been obtained at a reduced value of magnetic field. There was not sufficient drive power available to saturate the tube in this case, but about 100 kw output was obtained at a drive level somewhat below saturation. The output power again, was very constant across the 1250 to 1350 Mc band.

A brief attempt was made to operate the tube with the collector depressed. Under conditions that resulted in 28 percent efficiency without collector depression, the efficiency could only be increased to 32 percent with collector depression before the current returned to the circuit became excessive. It is not clear whether this low improvement factor is due to poor collector design or to the large space charge potential depression at the center of the high perveance beam. It would be quite difficult to design the first grounded cathode tubes so that they could be operated with the collector depressed, so the problem was not investigated further.

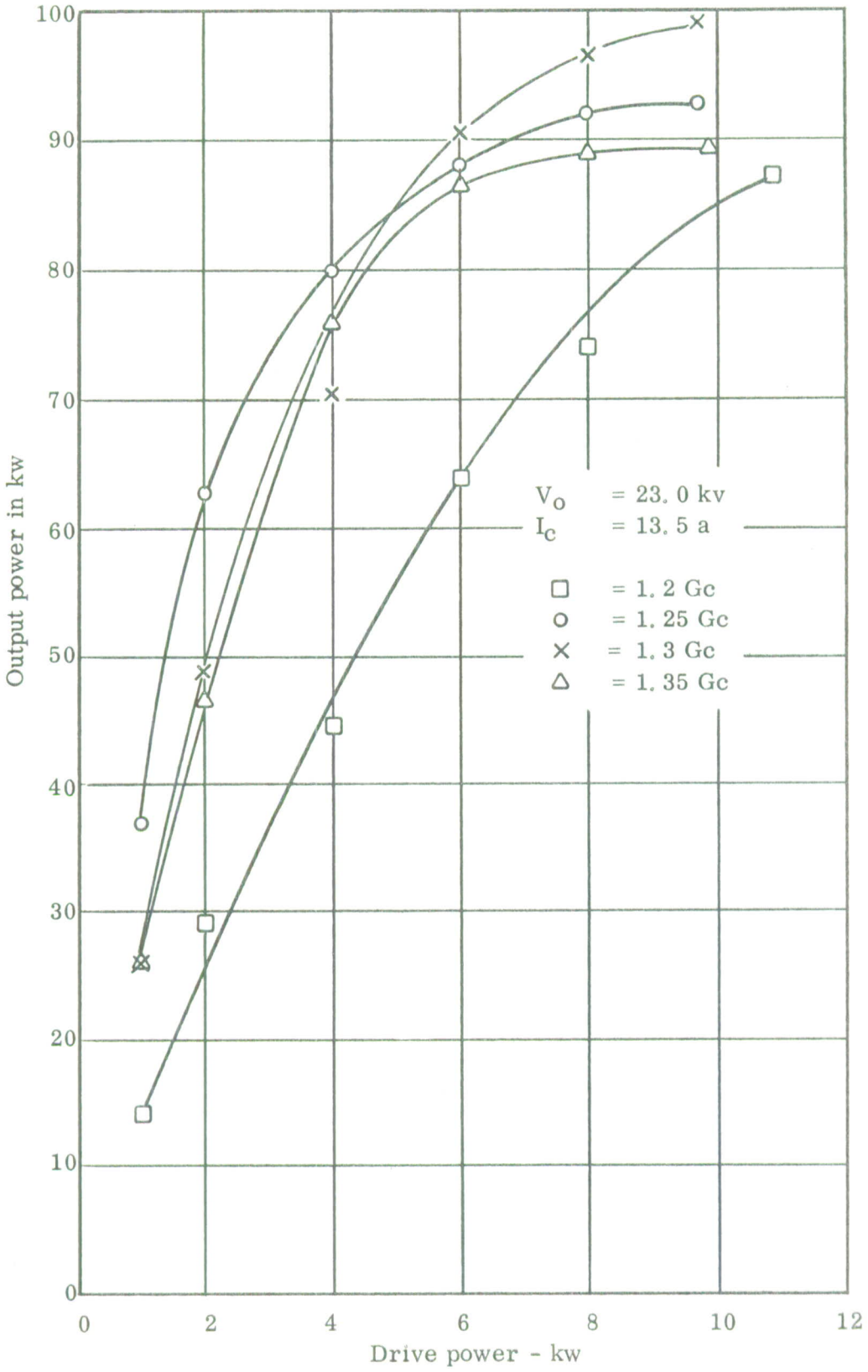

Fig. 20 - Power output versus power input curves at 23 kv and 13.5 amperes beam current for experimental tube no. 1. This tube was tested in a uniform magnetic field.

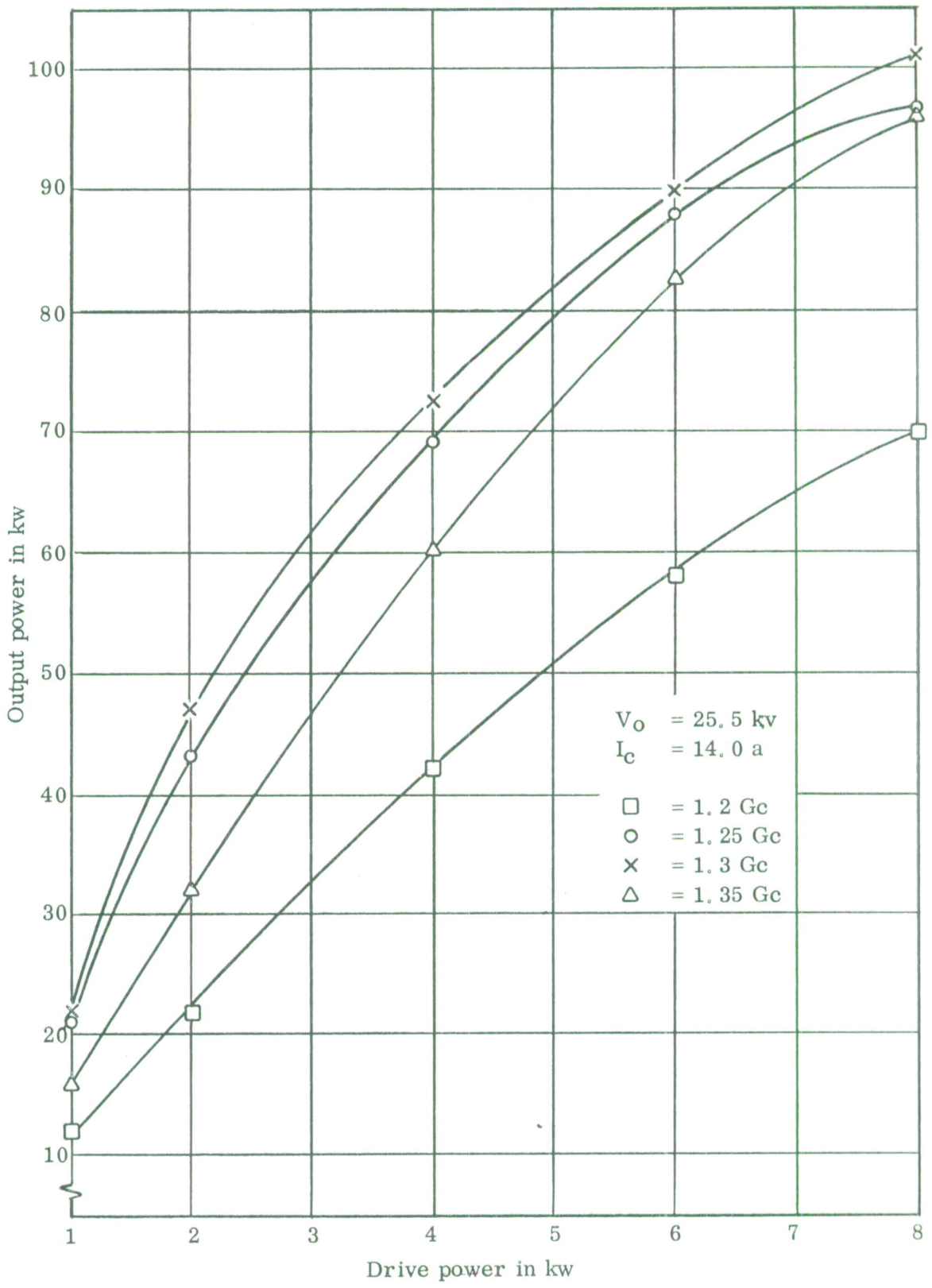

Fig. 21 - Power output versus power input curves at 25.5 kv and 14 amperes beam current for experimental tube no. 1. The available rf drive power was not sufficient to saturate the tube at this voltage.

The above results show that about 3 db additional gain is required. Increasing the circuit length by 0.8 inch will provide this gain. Beam efficiencies of about 30 percent or a little more can be expected without velocity tapering or a depressed collector. The tube appears to be stable without an internal attenuator with 10 db of large signal gain and the first grounded cathode tube will be constructed without an attenuator. The large signal tests were quite satisfactory.

Grounded Cathode Tubes and Beam Tester

Beam Tester

A beam tester of the grounded cathode type was constructed to evaluate the following:

1) The gridded perveance 5×10^{-6} electron gun which has a center post supporting the grid. The center post was added to the gun so that better grid cooling could be obtained. Using the center post allows copper to be used as the grid material. In tube No. 1 a moly grid with no center post was used.

2) Focusing of the grounded cathode type tube with no rf drive using a ppm magnet stack.

3) The arcing problem of the gun and circuit in a grounded cathode tube.

The tube exhibited some arcing but the problem was not severe. Focusing tests were carried out mainly at 23 kv because large signal tests on tube No. 1 indicated that 23 kv was a good operating point for the present circuit design. Beam transmission to the collector of a little over 96 percent was obtained at beam currents ranging from 12.5 to 14 amperes. The intercepted grid current is 22 percent of the cathode current. This is approximately equal to the shadow area of the grid and therefore is the expected value. The positive grid voltage swing required is 150-170 volts and the tests were conducted with a negative grid bias of 200 volts.

The magnets used in the above tests are Genox 6A material with an ID of 2.0 inches and an OD of 3.94 inches. Three complete periods were used and an auxiliary magnet was used at the gun end of the tube to approximately cancel the magnetic field in the gun region. A plot of the magnetic field as a function of axial position along the tube is given in Fig. 22.

The conclusion to be drawn from the above tests is that it is possible to periodically focus the tube without rf drive with a magnet diameter less than 4 inches. The grounded cathode gun design with the post through the center of the cathode appears to be satisfactory.

Ceramic Barrel Tube

The first grounded cathode tube constructed was the ceramic barrel tube. This tube has a ceramic barrel around the circuit. The ring-bar circuit and its supporting ceramics are brazed into the ceramic barrel. The ceramic barrel serves as a voltage insulator for the circuit which operates at about +23 kv. The circuit and its ceramic wedge support are shown in Fig. 23. The ceramic barrel with the circuit brazed in place is shown in Fig. 24. The perveance 5×10^{-6} gridded electron gun assembly is shown in Fig. 25. The collector assembly is shown in Fig. 26. The grounded cathode ceramic barrel tube is shown in Fig. 27 before final assembly.

The Gun

In this tube, a heat shield was added radially around the cathode. As a result, the heater power required was reduced from over 100 watts in previous tubes to about 65 watts. The grid interception current was also significantly reduced. For example, at 23 kv and 14.5 amperes total beam current, the grid interception current was only 3.6 amperes and the positive grid swing 180 volts. Previous tubes ran over 5 amperes grid current under similar conditions. A grid current of 3.6 amperes for a beam current of 14.5 amperes corresponds to grid interception of 20 percent of the cathode current and is about equal to the shadow area of the grid. The reduction in grid current is probably due to reduced emission from the sides of the cathode as a result of the added heat shield. A further reduction by about a factor of 2 would probably be possible with a modification of the grid mesh.

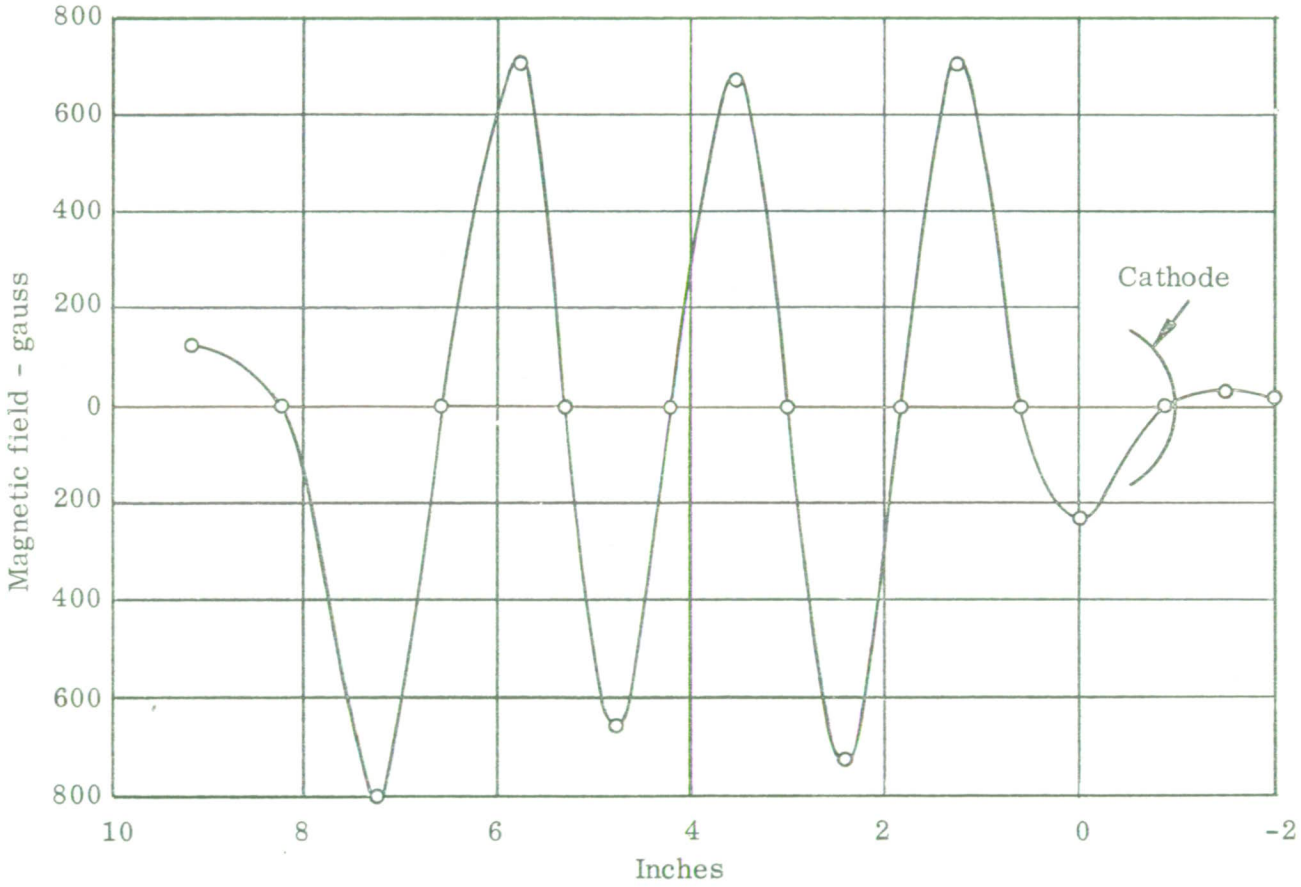

Fig. 22 - Magnetic field on the axis as a function of distance along the tube in the grounded cathode beam tester. The magnets were adjusted at the gun end of the tube for optimum focusing. Beam transmission of about 96 percent was achieved when the magnets were adjusted to provide approximately zero magnetic field at the cathode.

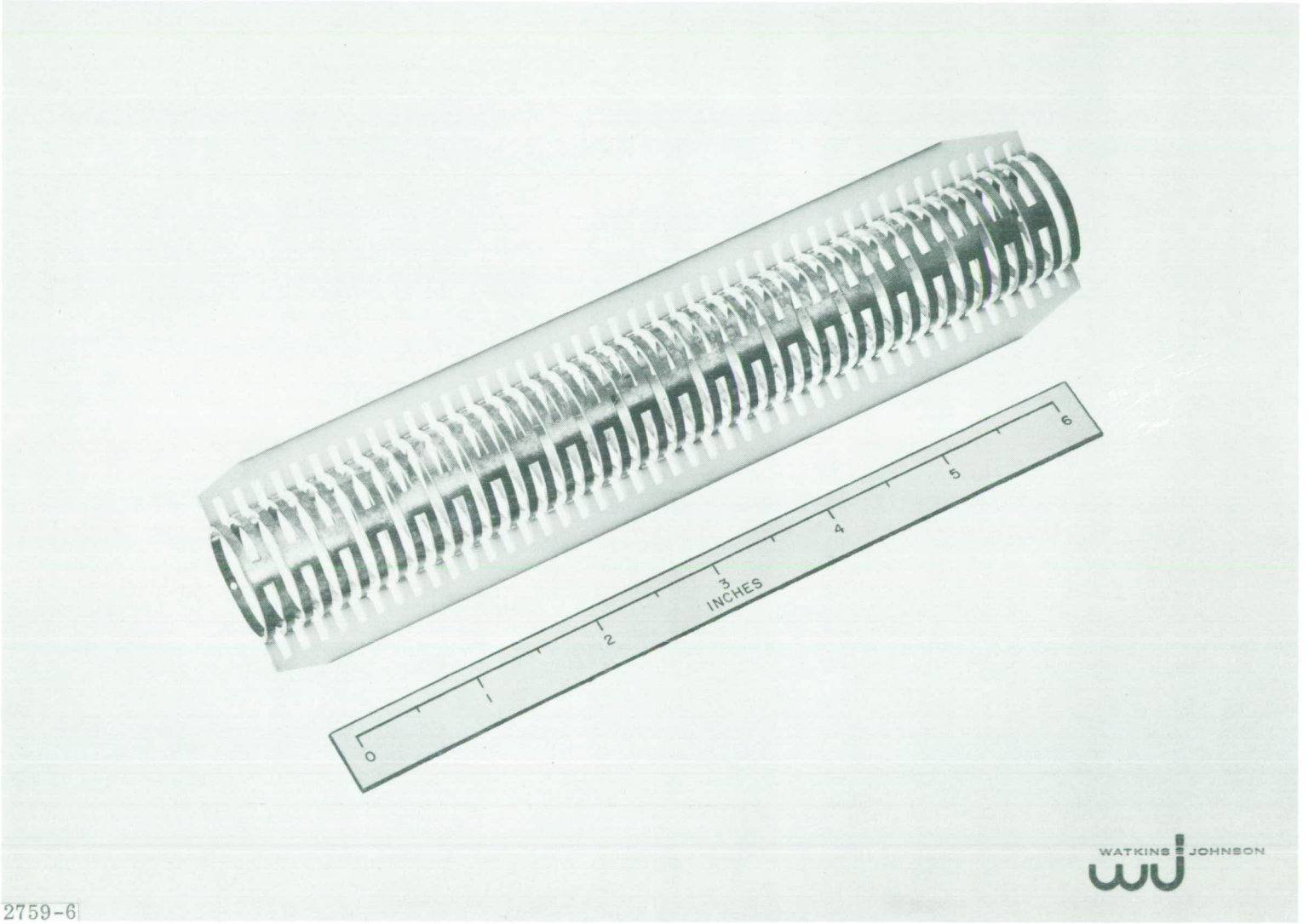

Fig. 23 - This photograph shows the copper ring-bar circuit and its supporting ceramic wedges. This assembly was brazed into the ceramic barrel of the first grounded cathode tube.

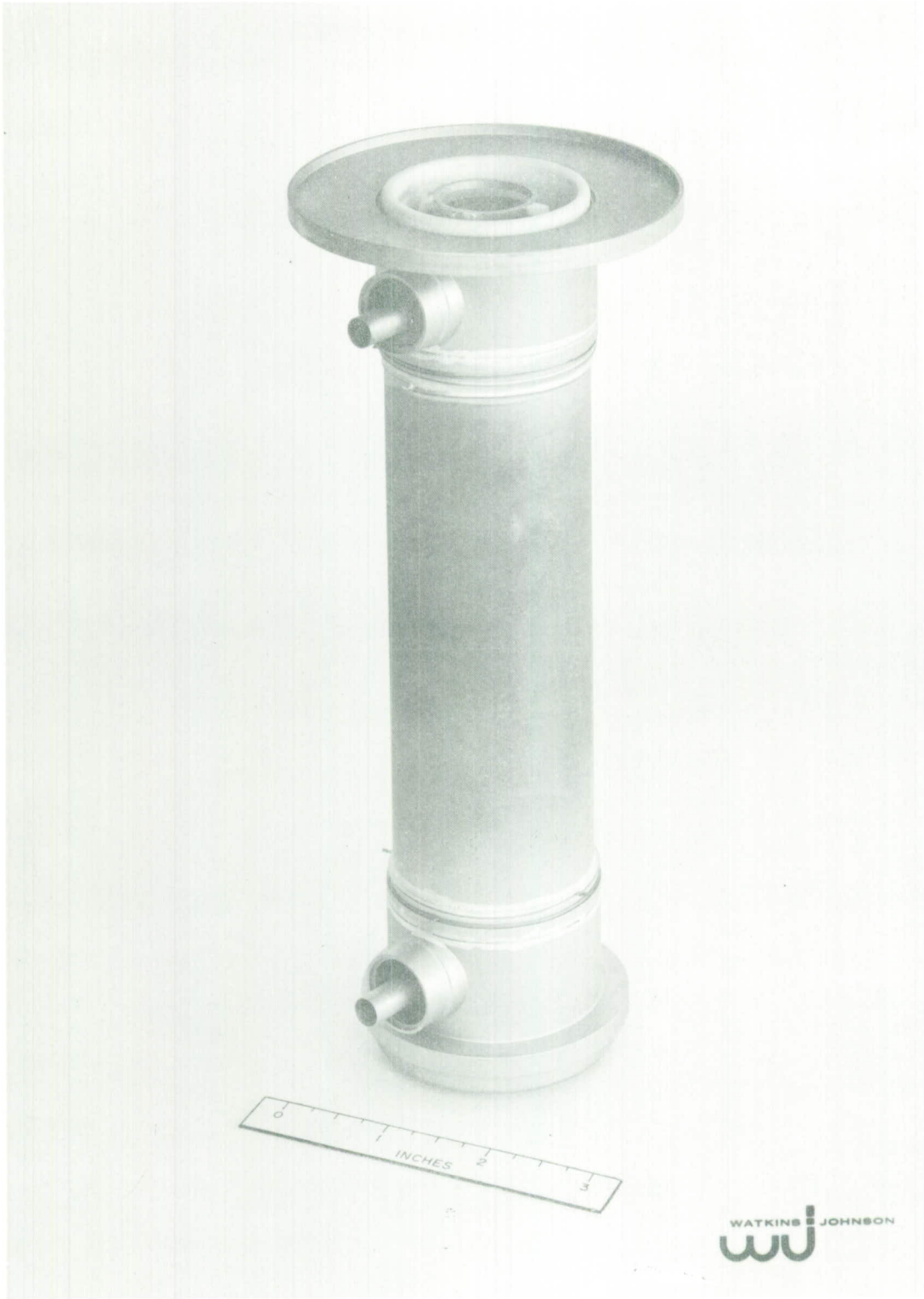

Fig. 24 - The photograph shows the ceramic barrel and circuit assembly as used in the first grounded cathode tube.

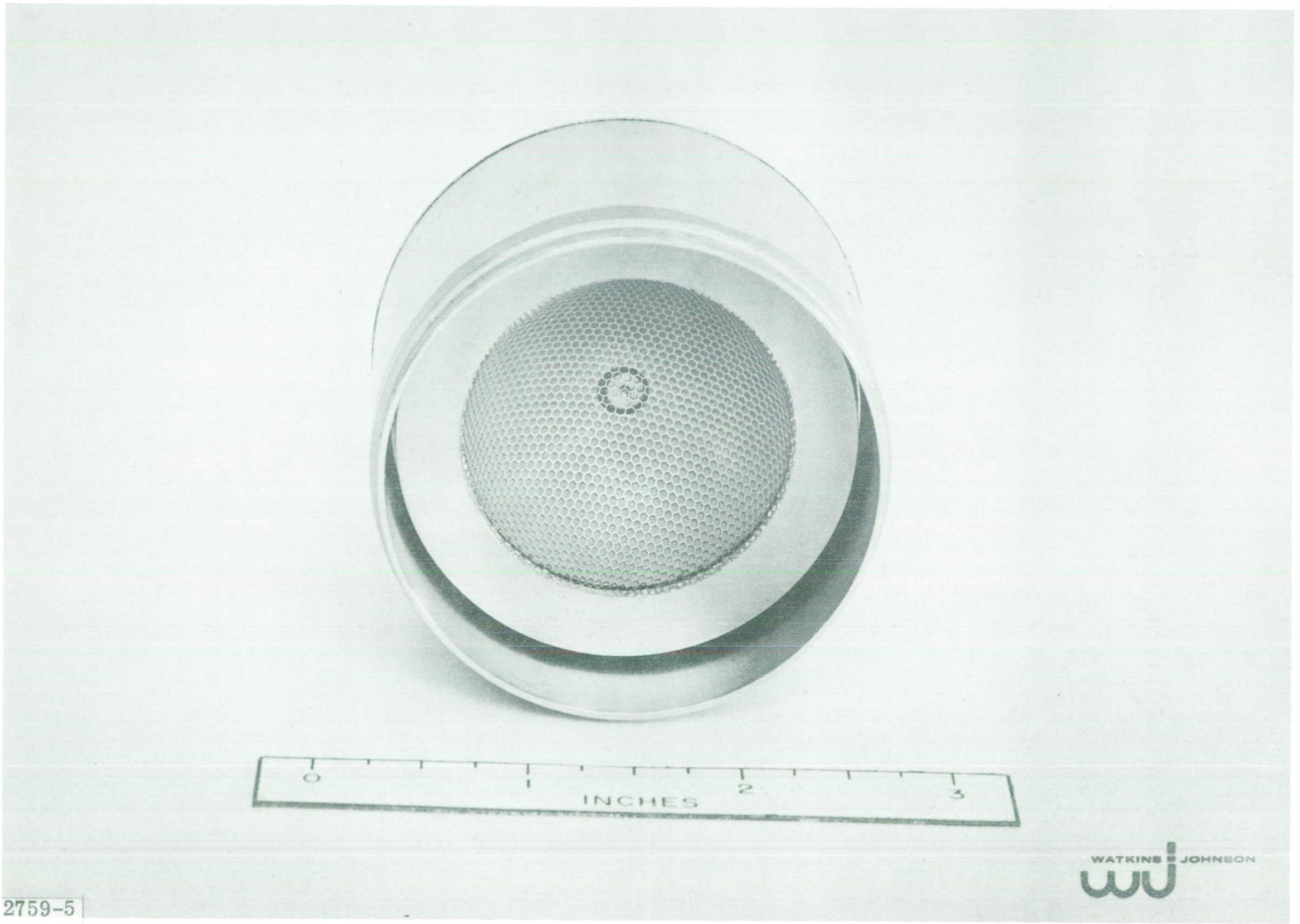

Fig. 25 - The gridded perveance 5×10^{-6} electron gun is shown in this photograph. The grid is supported by a center post in the center of the cathode for thermal and mechanical reasons. This gun assembly is used in both the grounded cathode tube.

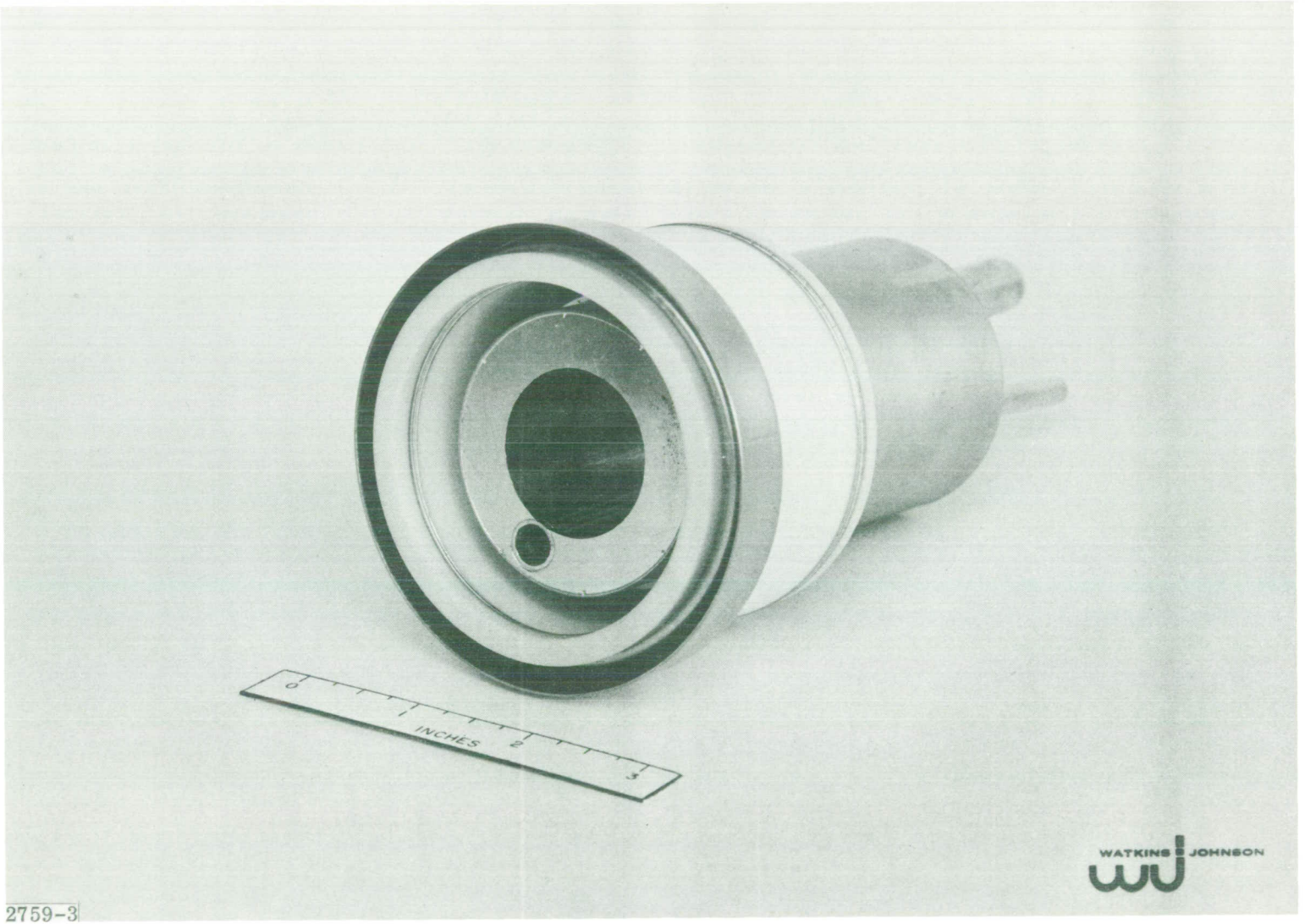

Fig. 26 - Collector assembly used on the grounded cathode tubes.

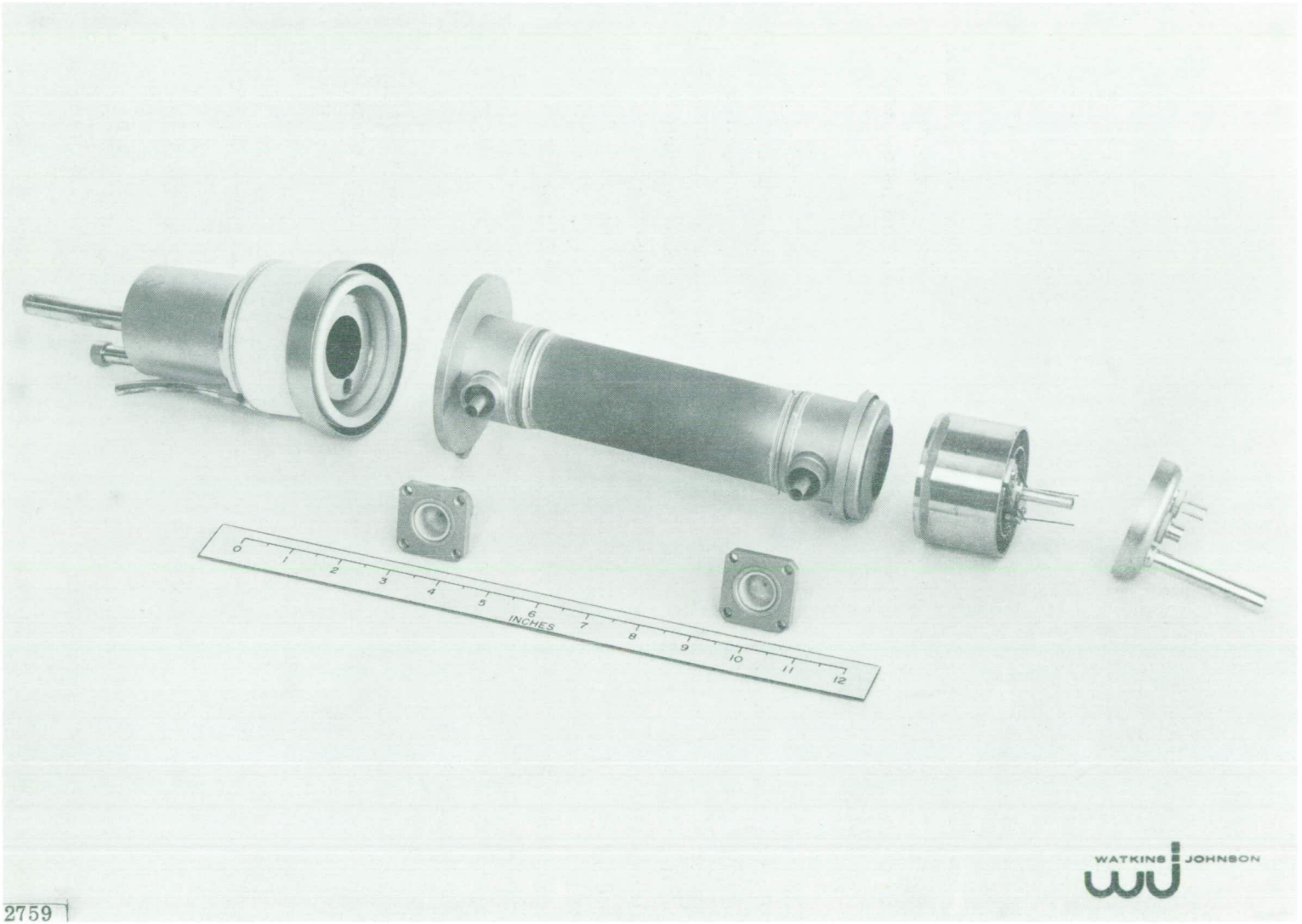

Fig. 27 - The grounded cathode tube shown with all its subassembly before final assembly.

RF Tests

Gain and power output measurements were carried out at low duty cycle. A great deal of difficulty was experienced with rf radiation from the collector. This was finally solved by enclosing the entire collector end of the tube in a box lined with aluminum foil and containing lossy material in the vicinity of the input leads to the circuit and collector. It was then possible to make consistent power readings although there was still some difficulty experienced in reading the circuit and collector currents. Under certain conditions, the rf would modify the current readings. Similar difficulties can be expected in an actual system and it will be necessary to shield the collector and high voltage leads appropriately.

RF tests were conducted under a variety of focusing conditions. Extreme rf beam defocusing was experienced under all focusing conditions except with a rather large uniform field from an electromagnet. Unfortunately, it was not possible to obtain good transmission with the electromagnet even in the absence of rf because of magnetic leakage into the gun region. The data that will be presented was obtained with a periodic focusing system with a period of 2.25 inches and a peak magnetic field on the axis of about 650 gauss. The defocusing with rf was extremely bad, becoming noticeable at about 5 kw output and increasing until beam transmission was only 30 - 40 percent at power outputs of 75 - 100 kw. The focusing problem will be discussed in a following section.

Fig. 28 is a plot of small signal gain versus frequency for 24 kv and 13.75 amperes beam current, and for 23 kv and 13.35 amperes beam current. These curves were taken at a few hundred watts drive power which results in some beam defocusing. The data is not strictly small signal but the gain value of about 19 db is probably correct. 19 db is the design value for small signal gain. The measured gain variation as a function of frequency is probably due to errors in the calibration of couplers and attenuators or to a mismatch external to the tube. It is not due to tube mismatch because the period of the variation is less than 4 percent in frequency which would correspond to a line length between mismatches of over 13 wavelengths. The tube is less than 4 wavelengths long.

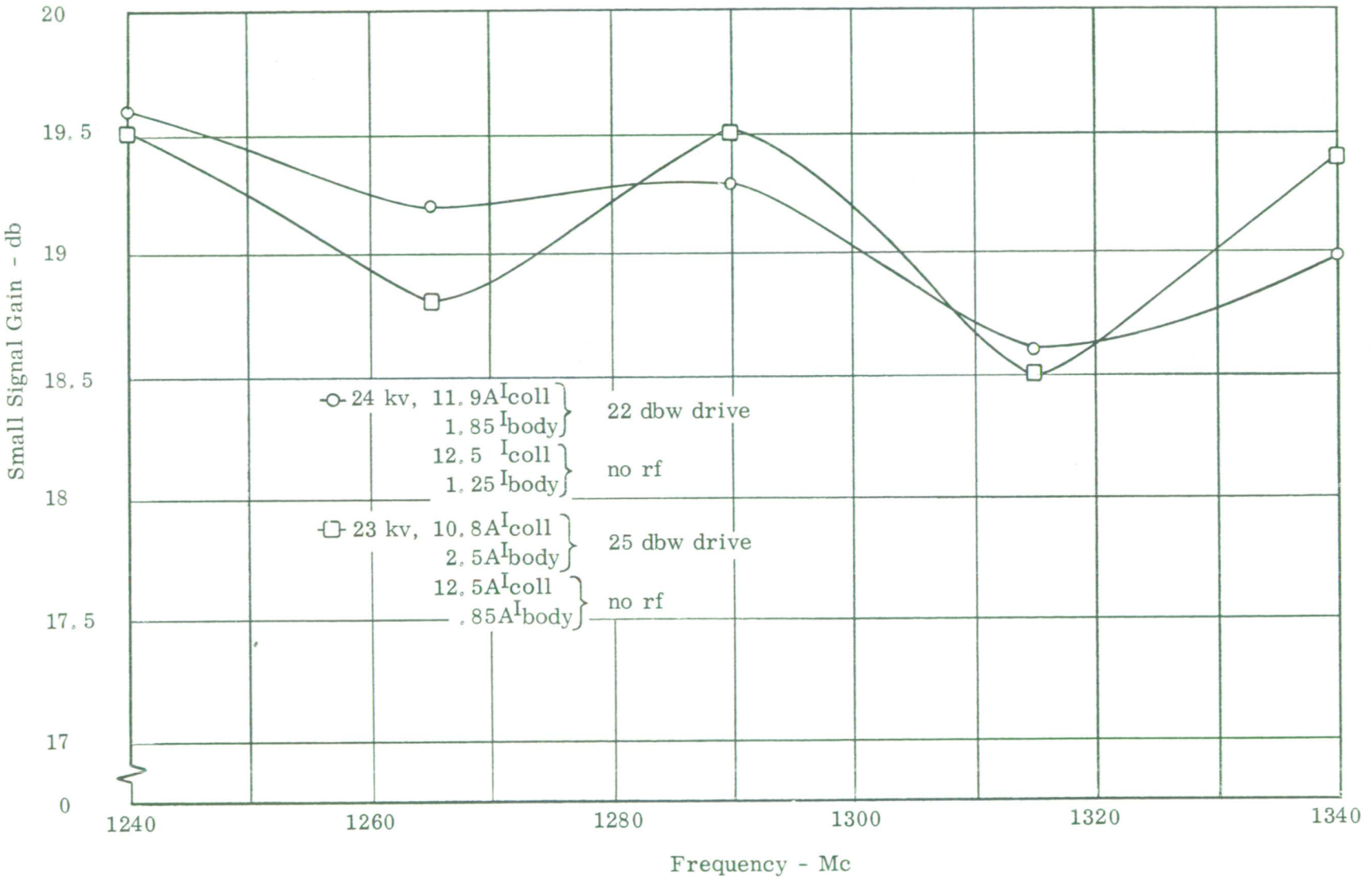

Fig. 28 – Small signal gain as a function of frequency. The gain variations are believed to be due to effects external to the tube.

Power output as a function of drive power is plotted if Figs. 29, 30, and 31 for different voltages and beam currents. The saturation characteristics are very uniform as a function of frequency. However, saturation occurs very gradually and the output power is a little lower than was obtained from the original grounded circuit tube which was tested in an electromagnet. A single curve from tube No. 1 is plotted on Fig. 30 for comparison purposes. The small signal gain is lower but saturation is not as gradual and the peak output power is higher. The gradual saturation characteristics and the somewhat reduced output power of tube No. 2 are probably due to the extreme rf defocusing that occurred.

Beam Focusing

Figs. 32, 33, and 34 show beam transmission as a function of rf output power for the three cases shown in Figs. 29, 30, and 31. These sets of curves are virtually identical. Transmission is essentially unaffected until the output power reaches about 10 kw. Transmission then decreases very rapidly with output power to a value of about 30 - 40 percent at output powers of 75 kw or so. This behavior indicates that the period of the magnetic field is probably too long. As soon as enough power is extracted from the beam to slow some of the electrons a little, the transmission decreases. For a fixed beam current density, the period of the magnetic focusing system is proportional to the velocity to the three halves power so that the required period for stable focusing decreases as the electron velocity decreases. The structure we have been using seems to be almost marginally stable and a very slight decrease in electron velocity results in poor focusing. It would be desirable to decrease the magnetic period from 2.25 inches to 1.5 inches. The peak value of magnetic field in our focusing system is also a little low. The peak value is 650 gauss whereas about 810 gauss would probably give good focusing.

Attempts have been made to focus the tube with various different schemes. The period was increased to 2.75 inches from 2.25 inches. The peak field increased to 850 gauss and fairly good focusing was obtained without rf. However, with rf, defocusing was again very bad. A single reversal magnet system was tried. It was only possible to achieve about 65 percent transmission without rf, probably because of magnetic leakage into the gun region. Defocusing with rf was again

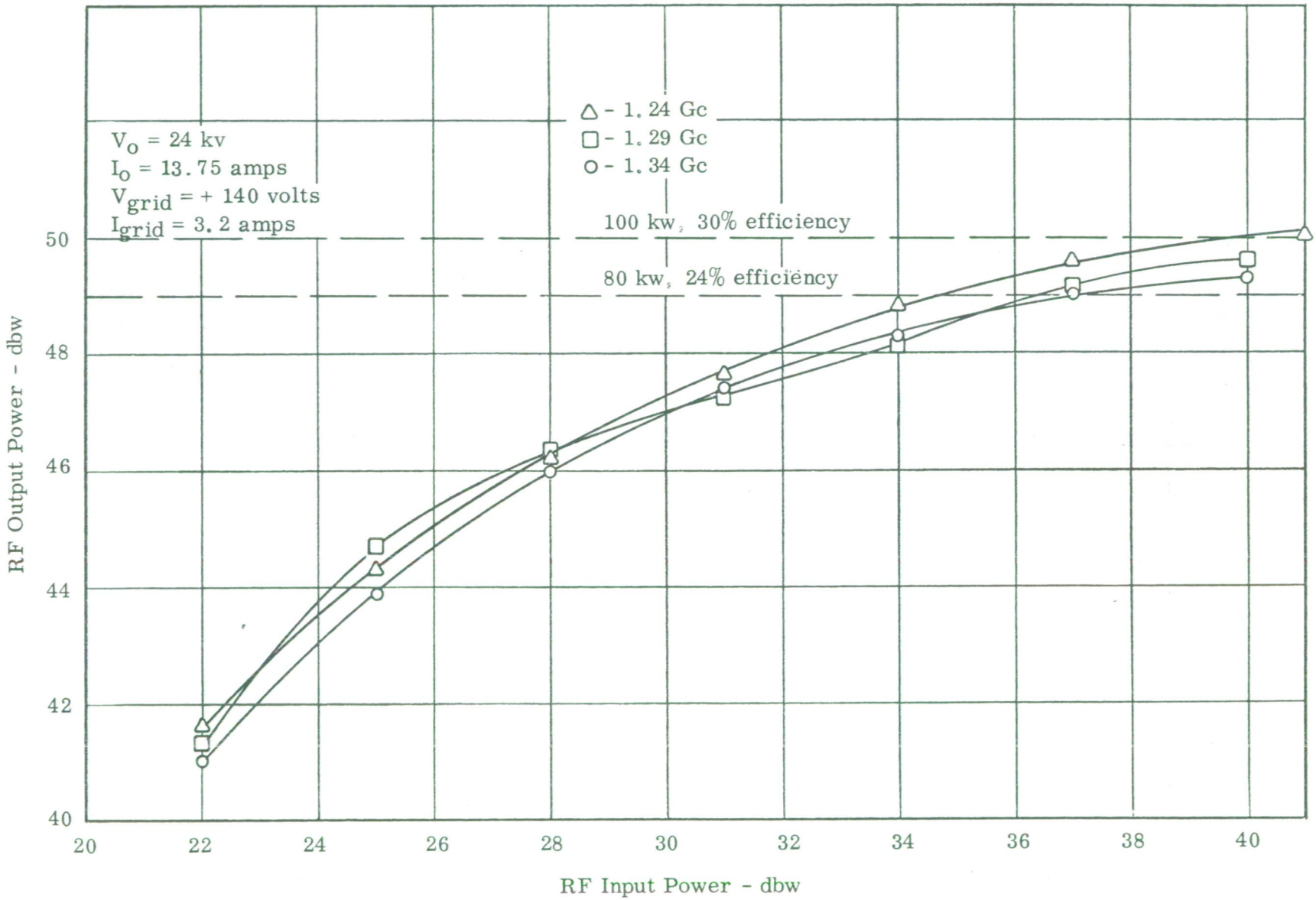

Fig. 29 – Saturation curves for 24 kv beam voltage, 13.75 amperes beam current. The gradual saturation and low efficiency is believed to be due to extreme rf defocusing.

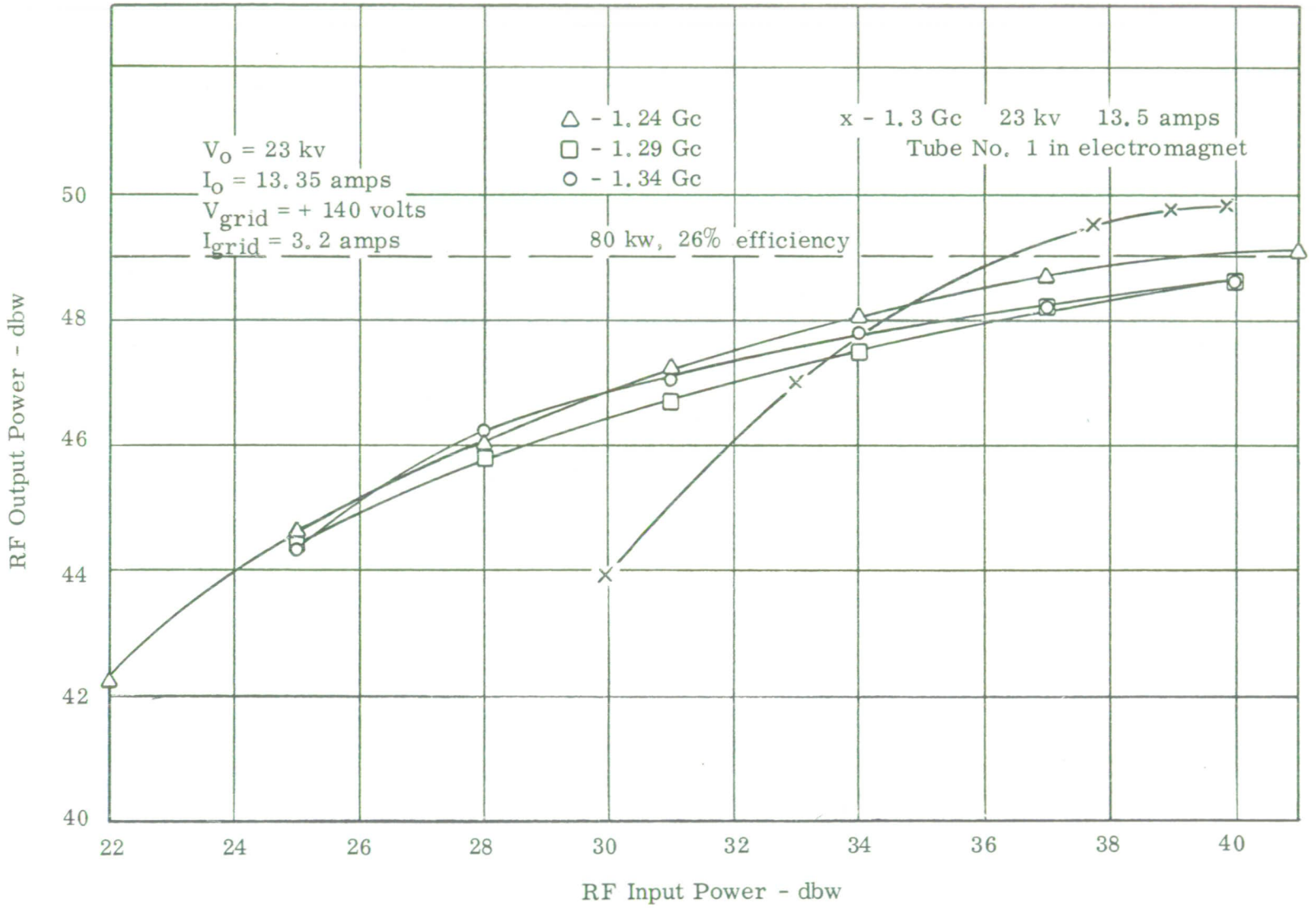

Fig. 30 - Saturation curves at 23 kv. A curve for the grounded circuit tube which was operated in an electromagnet with very little defocusing is shown for comparison. Saturation occurs more quickly and the efficiency is higher.

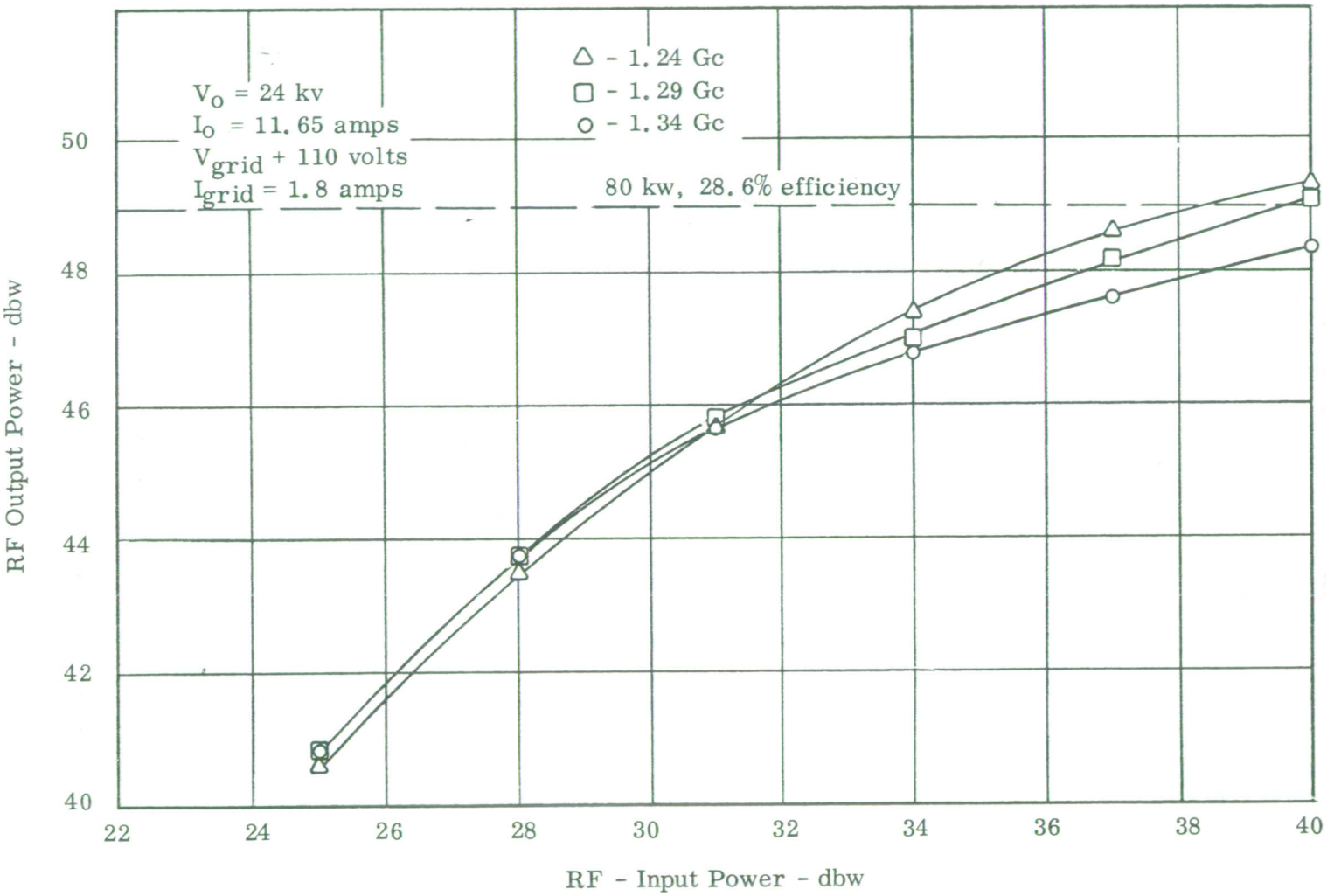

Fig. 31 - Saturation curves at 24 kv but reduced beam current. The small signal gain is only about 16 db.

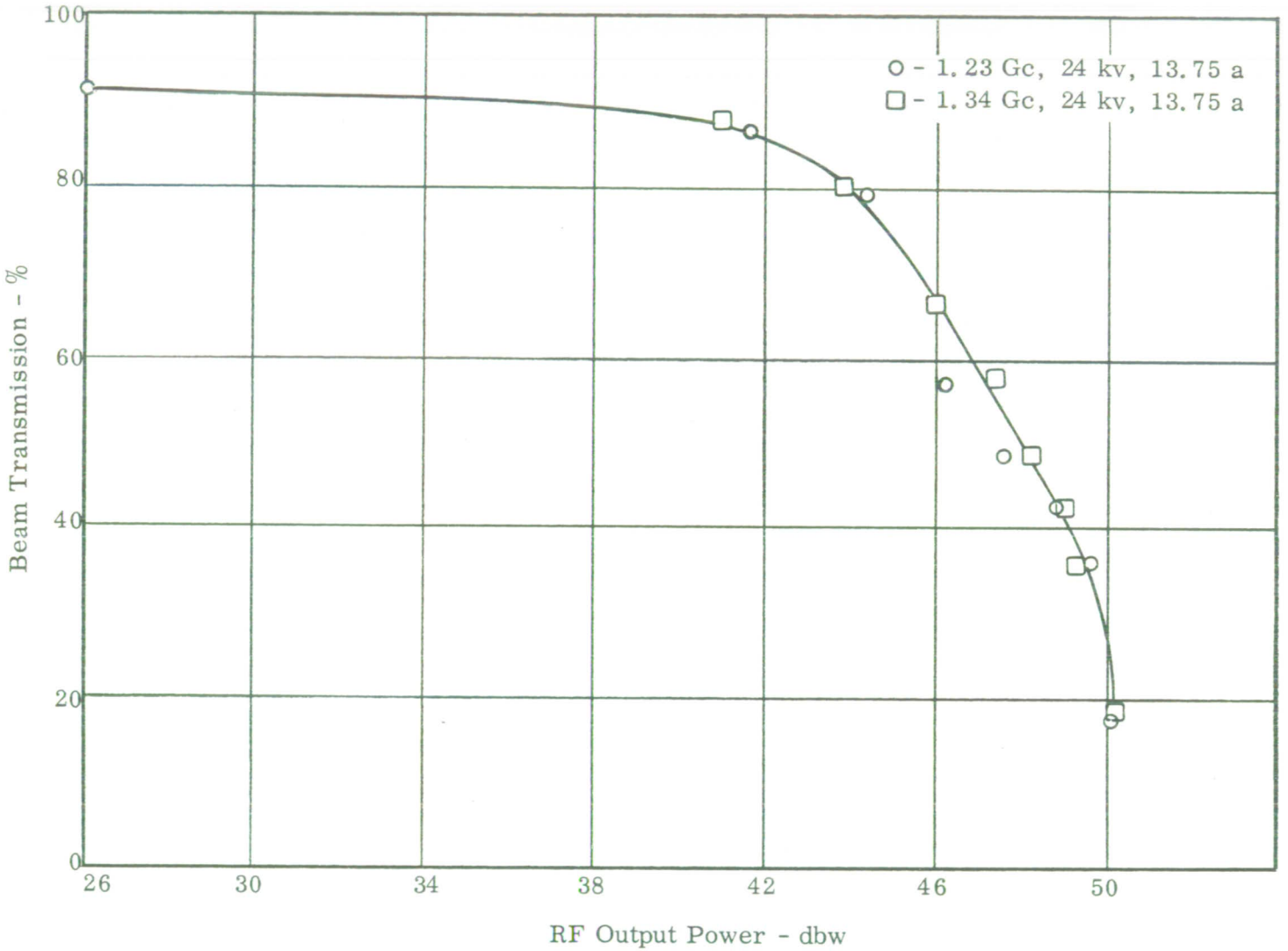

Fig. 32 - Beam transmission as a function of rf output power at 24 kv. The extreme defocusing is probably due to a combination of too long a magnetic period and too weak peak field.

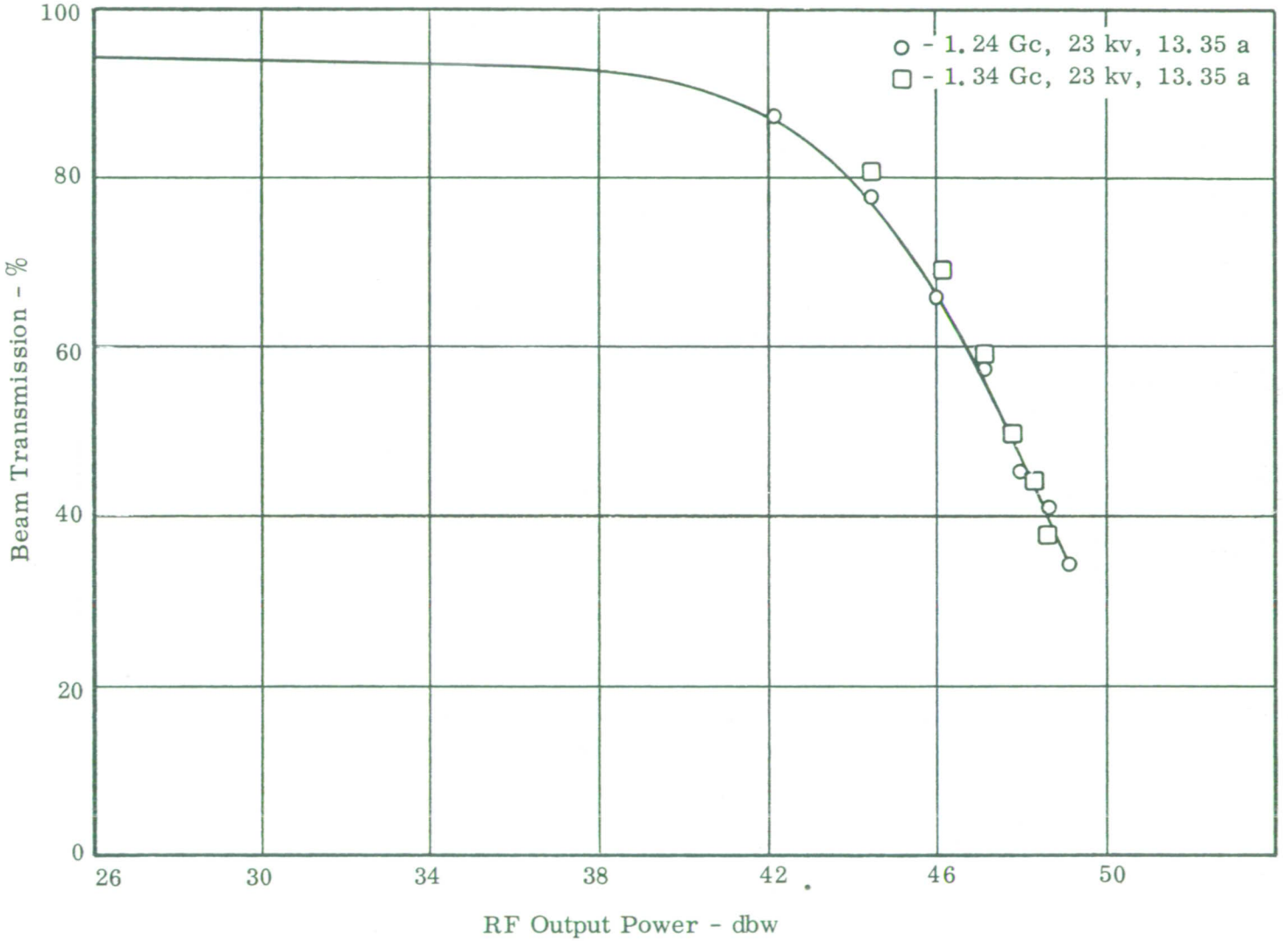

Fig. 35 - RF defocusing at 23 kv. The curve is almost identical to the curve for 24 kv.

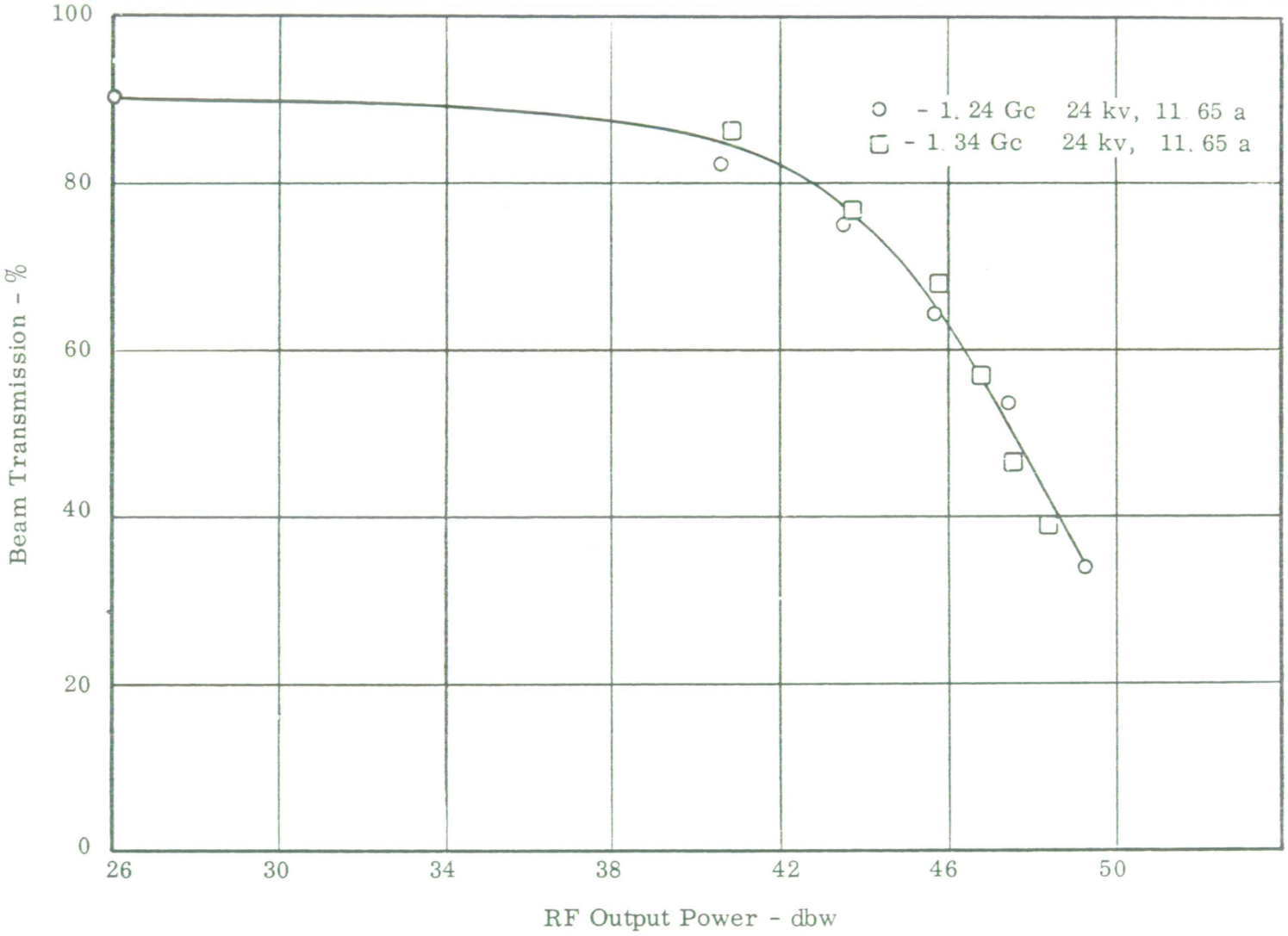

Fig. 34 - RF defocusing at 24 kv and reduced current. Defocusing is still almost the same as for the previous two cases.

very bad. However, the magnetic field was much lower than could actually be achieved with an optimum single reversal stack. Fig. 35 is a photograph of the tube used in the above test.

The ceramic barrel grounded cathode tube was tested with single reversal magnetic fields. The magnetic field shown by the solid line in Fig. 36 was tried first. 93 percent transmission was obtained without rf drive and 70 percent transmission with saturated rf drive. To improve beam transmission at saturation, a second magnetic stack was made up with the magnetic field as shown by the dashed line in Fig. 36. This second configuration has a stronger magnetic field at the output of the tube. By increasing the magnetic field in this region of the tube transmission improved from 60 percent to 75 percent under rf drive. The gain was 12-13 db over the frequency band and power output was approximately 80 kilowatts over the band.

Metallic Barrel Tube

A very considerable amount of difficulty was encountered with the ceramic barrel used in the present tube has led us to a design which utilizes a stainless steel barrel. The circuit will be supported by means of two ceramic rods which have a cross-section in the shape of a cross. One leg of the cross is brazed to the steel barrel and the opposite leg is brazed to the circuit. The other two legs of the cross increase the surface distance between high voltage points and form a potential barrier. Fig. 37 shows this assembly. This assembly was tested to 35 kv in a bell jar without arcing. Fig. 38 is a photograph of the metal barrel and circuit assembly. Fig. 39 is a photograph of the metal barrel grounded cathode tube, the test results of which are described below.

The metal barrel tube was tested with these results. The tube operated without arcing with voltages up to 30 kv with a cold cathode. The tube arced consistently at about 10 kv with beam current on. Several days were spent trying to increase the operating voltage so that rf and focusing data could be obtained. It was decided to remove the tube from the modulator and operate the vac-ion pump while drawing cathode current to improve the tube vacuum before further tests on the modulator are attempted. The arcing difficulty may also have been associated to some extent with the crack in one of the ring bar circuit shopping ceramics. The tube also had a leakage of 25 megohms between the circuit and ground. This most likely is due to the cracked ceramic supporting wedge.

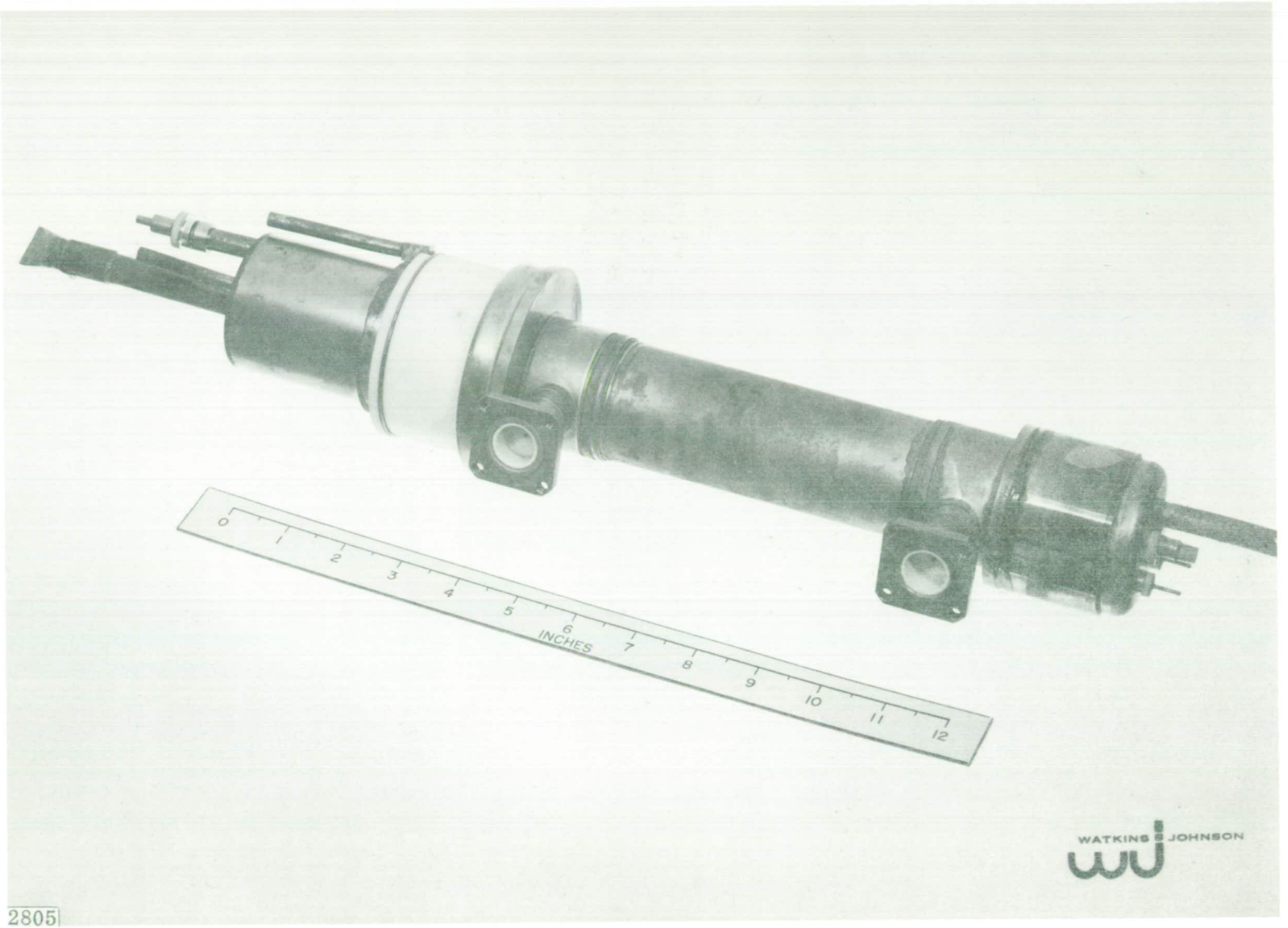

Fig. 35 - The grounded cathode experimental tube with ceramic barrel.

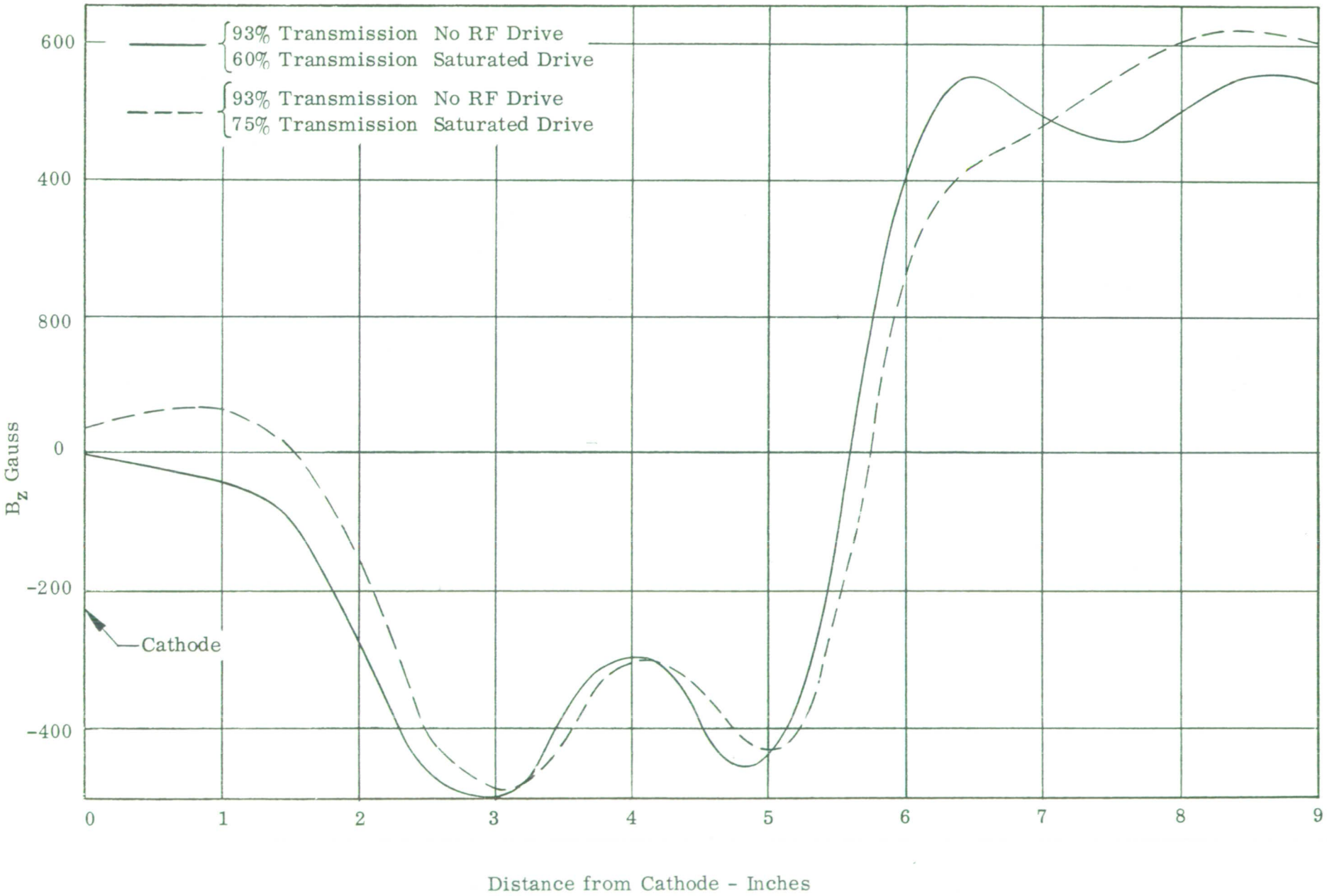

Fig. 36 - The graph shows two similar magnetic fields used to focus the grounded cathode tube. Both fields resulted in 93 percent transmission with no RF drive. Under full RF drive the field shown by the dashed line resulted in higher transmission due to the strongest magnetic field over the output of the tube.

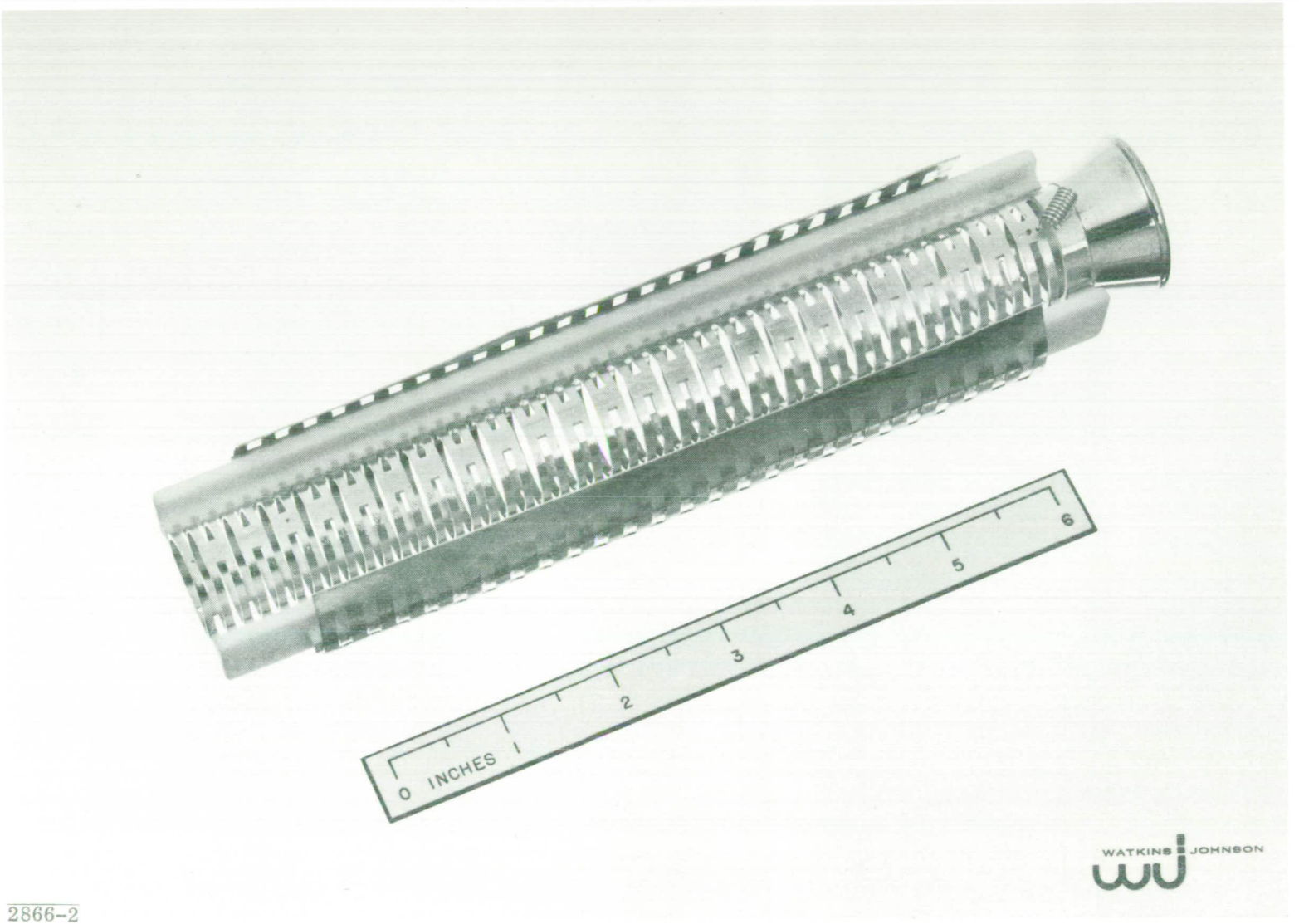

2866-2

Fig. 37 - Ring-bar structure mounted on cross-shaped ceramic wedges for use with a metal barrel. This assembly has successfully withstood 35 kv dc in a bell jar test.

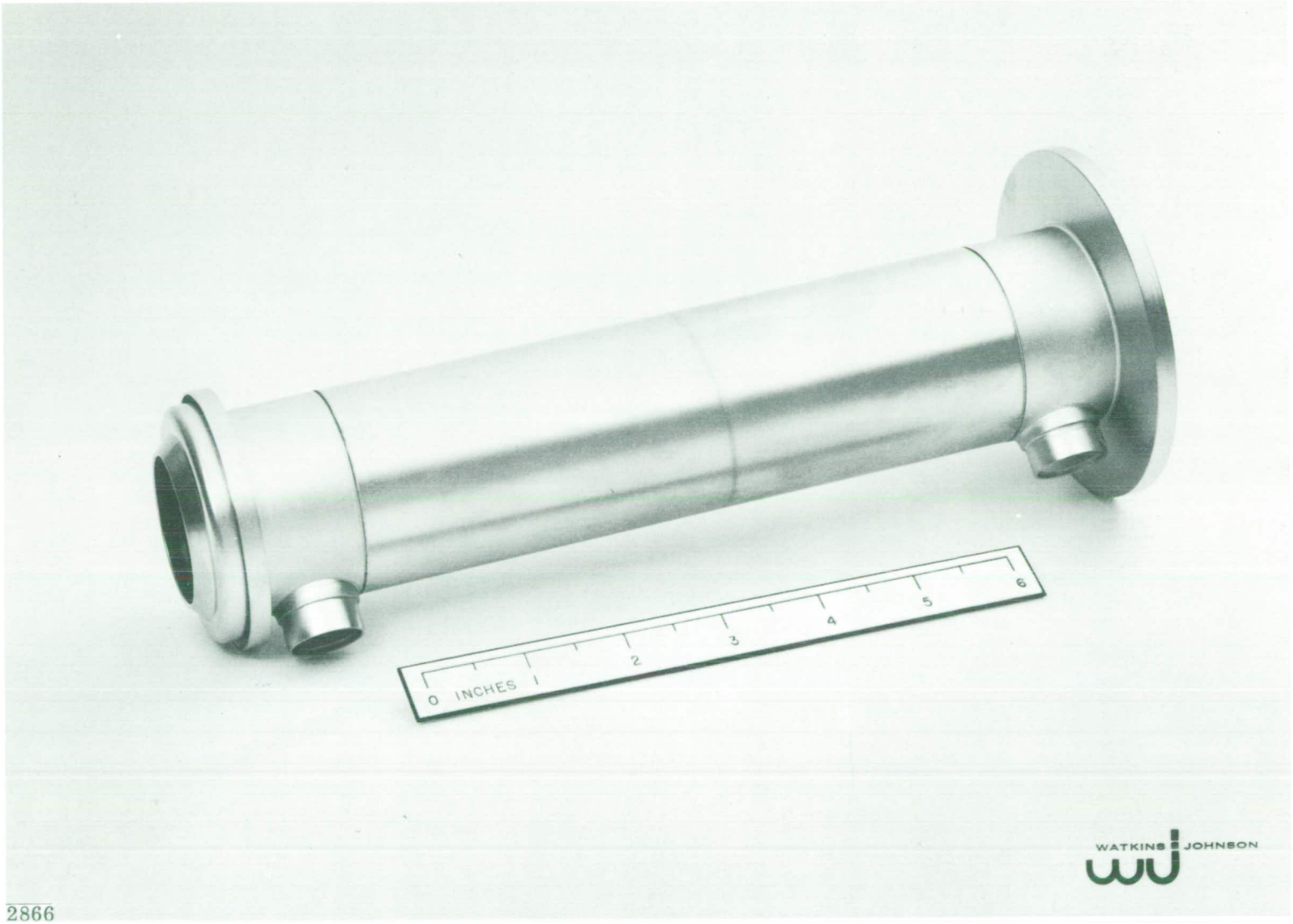

Fig. 38 - Metal barrel assembly for the grounded cathode tube.

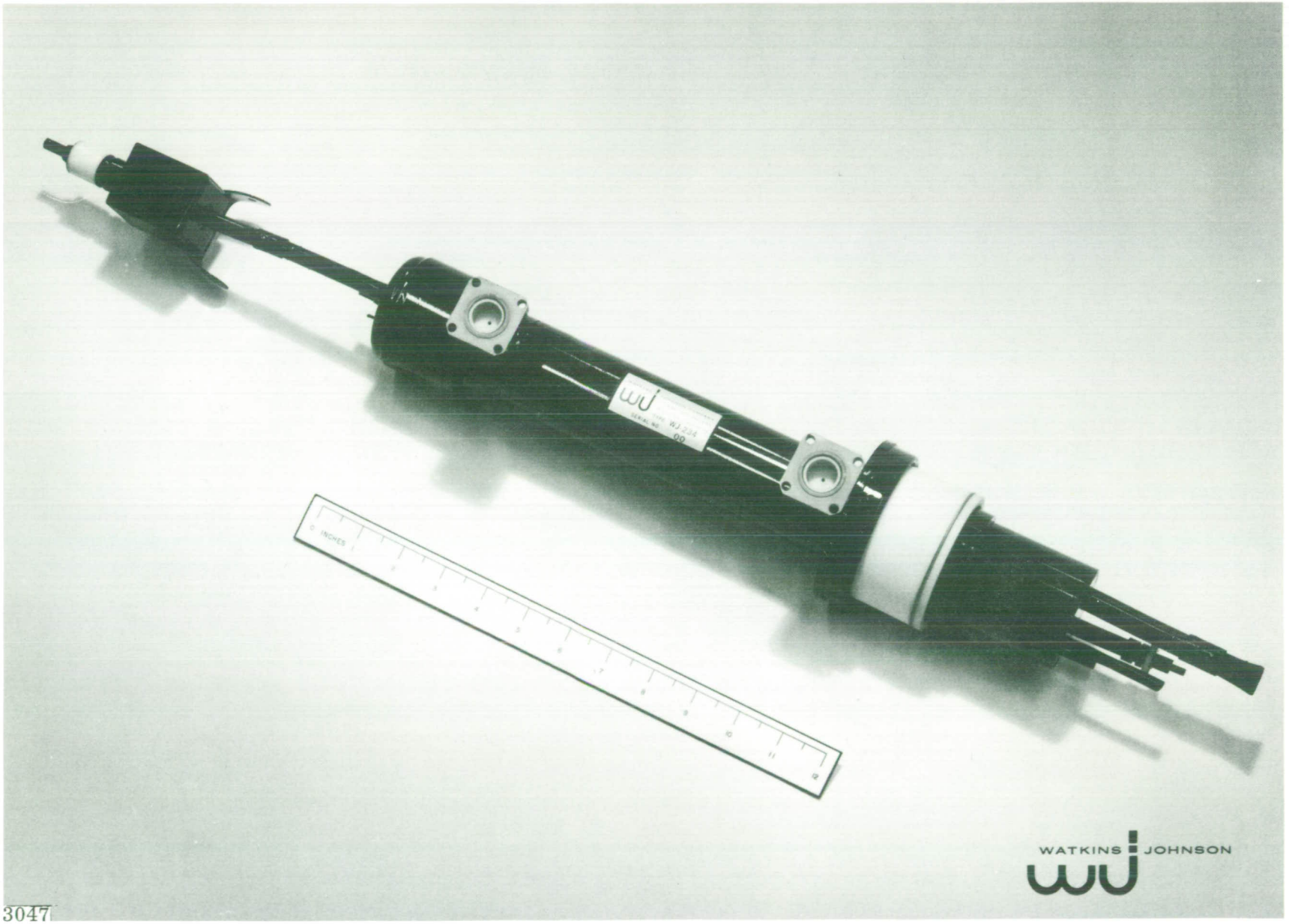

3047

Photograph of metal barrel grounded cathode tube.

The grounded cathode metal barrel tube was operated for a number of days at 1000 volts and 50 milliamperes of CW beam current to improve pressure. The tube was then tested on the modulator. This tube had earlier arced at 10 kv. After the tube had been cleaned up it operated up to 23 kv without serious arcing. The beam was focused with a single reversal magnet. The results similar to those obtained with the ceramic barrel grounded cathode tube for both rf and focusing.

SUMMARIES AND CONCLUSIONS

Summary of Tube Focusing

Several different types of focusing structures have been tried on the 100 kilowatt traveling-wave tube. Best results were obtained using the grounded circuit tube in a solenoid. This resulted in 96 percent transmission without rf drive. A beam transmission of 88 percent was measured with rf drive at a magnetic field of 630 gauss.

A second method of focusing the tube was to use a PPM magnet stack. This resulted in 96 percent beam transmission with no rf drive. Transmission was essentially unaffected by rf drive power until the output power of the tube reached 10 kilowatts. Transmission then decreased very rapidly with output power to a value of 30 to 40 percent at output powers in the order of 75 kilowatts. The experimental results using the solenoid indicate that a periodic focusing system of about 810 gauss peak field with a period of 1.5" or less would be required if any satisfactory results could be expected in the presence of rf. It is impossible to obtain the required field with any available ceramic magnets when the period of the PPM stack is 1.5". For this reason the periodic focusing system was abandoned.

A single reversal focusing system was then tried. The single reversal magnetic field resulted in 93 percent beam transmission without rf drive and 75 percent beam transmission under saturated rf drive. Many different magnet stacks were placed on the tube. In each case best results were obtained with field configurations that were very similar. The reversal always seemed to optimize the transmission when it occurred at approximately the same locations relative to the cathode. Similar results were observed when a problem was studied on the analog computer at Stanford. The reason for this optimum reversal location always occurring at the same spot is due to the fact that the tube is only about four scalloping wavelengths long; therefore the reversal must occur where the beam has the proper inward scalloping. This always occurred approximately the same distance from the start of a magnetic field. It was observed that rf defocusing occurs when output power is 10 db below saturation using a PPM magnet stack. This immediately indicates that the rf defocusing may be due to beam modulation at the reversal. It is impossible to move the reversal point on the 100 kilowatt grounded cathode tube to determine the exact effect of beam modulation at the reversal and rf defocusing.

From the results to date, it appears that a straight field PM focusing system would result in the best defocusing characteristics for the tube. It would be expected that beam transmission under rf drive would be in the neighborhood of 88 percent which is the value obtained using a solenoid. The straight field permanent magnet would have two basic disadvantages. 1) The external leakage fields would be very large. 2) The magnet weight would be somewhat larger than in the case of PPM or single reversal magnet stacks.

Summary of the Program

The grounded circuit tube which was the first tube built on the program produced 100 kilowatts of rf power and had efficiencies of over 30 percent. This tube was slightly low in gain but this is because the circuit was shorter than the circuits used in the grounded cathode tube. This tube focused very well in a solenoid and should also be capable of similar focusing and rf results when focused in a straight field permanent magnet.

The grounded cathode tube design utilizing a ceramic barrel appears to be reasonably satisfactory from an electrical point of view. The tube has been tested over a period of ten months with some arcing but probably not a serious amount. It is reasonable to expect that further improvements over a period of development and production would reduce the arc count to an acceptable level.

The gridded gun operates satisfactorily at low duty cycle. Problems associated with grid expansion could develop at full duty cycle but it does not seem that these problems would be serious. Grid cutoff characteristics are such that it would be possible to reduce the grid current to about 10 percent of the cathode current without increasing the total grid voltage swing to more than 500 volts. This would be accomplished by obtaining a more open grid mesh and possibly by reducing the size of the wires. This has not been done.

The capacitively coupled rf windows are completely satisfactory at low duty cycle and no serious problem is anticipated at full duty cycle.

The efficiency and gain of the tube are probably satisfactory. The poor focusing under rf drive has made it a little difficult to evaluate the results. However, the small signal gain is correct and the efficiency only slightly lower than was achieved previously with good focusing on the grounded circuit tube.

The circuit support ceramics are made from alumina at present. Alumina will not be satisfactory at full duty cycle even if reasonably good transmission is achieved. The original beryllia slabs proved to be completely unsatisfactory because the mechanical strength of the particular material used was very low. The difficulties experienced with focusing have prevented us from ordering more beryllia until the tube design becomes firm.

The metal barrel tube with the grounded cathode is the more desirable design because it is possible to extend the length of the tube almost arbitrarily and the tube would be much more rugged. This tube was only tested briefly but has the same electrical properties as the ceramic barrel tube.

REFERENCES

1. Branch, G. M. and Mihran, T. G. Trans. PGED ED-2 No. 2 3-11 (1955)

2. Birdsall, C. K. and Brewer, G. R, Hughes Research Laboratories. Technical Memorandum No. 396, "Traveling Wave Tube Propagation Constants for Finite Value of C" 23 June 1955

3. Beam, W. R. and Blattner, D. J., RCA Review March 1956 "Phase Angle Distortion in Traveling-Wave Tubes".

APPENDIX I

TEMPERATURE RISE CALCULATIONS OF THE RING-BAR CIRCUIT ASSEMBLY

Data used to calculate temperature rise of ring-bar circuit assembly.

Average rf power of tube	1 kw
Beam efficiency	30 percent
O.D. of ring-bar circuit	.93 inch
I.D. of ring-bar circuit	.83 inch
Width of ring	.072 inch
Guide wavelength of ring-bar circuit	2 inches at 1.3 Gc
Pitch of ring-bar	.312 inch
Rings per pitch	2
RF loss of circuit	1 db ~ 1/4 db per guide wavelength

Ring-bar circuit is supported as shown in Fig. 1 by two ceramic wedges of beryllia.

Specific heat conductivity = K

For copper $K = 3.88 \ \frac{\text{watts}}{\text{cm } ^{o}\text{C}}$

For beryllia $K = 2.5 - 4 \times 10^{-3} T \ \frac{\text{watts}}{\text{cm } ^{o}\text{C}}$ (See Fig. 10)

CALCULATION - REGION 1 (See Fig. 8)

Assume the following:

1. $T_1 = 40^{o}C$ (edge of wedge is cooled) at all power levels.
2. Cross-sectional area is a function of distance from the edge of the wedge.

$$A = A(L) = (b-a)\, t \, \frac{L}{L_o} + at \quad \text{(See Fig. 8)}$$

Use the temperature drop equation

$$\Delta T = \frac{WL}{KA}$$

where

ΔT = degrees centigrade
W = power flow in watts
A = cross-sectional area in cm^2

K = specific heat conductivity in $\frac{watt}{cm - c^o}$

For region 1, A is a function of L and K is a function of T when beryllia is used. The temperature drop equation takes the following form.

$$-dT = \frac{W\,dL}{A(L)\,KT}$$

For beryllia $K(T) = 2.5 - 4 \times 10^{-3} T$ (See Fig. 2)

$$A(L) = (b-a)t\,\frac{L}{Lo} + at$$

a = .072 inch
b = .154 inch
Lo = .170 inch
t = .125 inch

} See Fig. 1

$$A(L) = (.058 + .153\,L)\ cm^2 \text{ where L is in cm}$$

Intergrating the temperature drop equation from T_2 to T_1 and from to O to L_o one obtains the following equation.

$$2.5\,(T_2 - T_1) - 2 \times 10^{-3}\,(T_2^2 - T_1^2) = 4.94\,W$$

This equation reduces to the following when $T_1 = 40^oC$

$$T_2^2 - 1250\,T_2 + 48400 + 2470W = O$$

Solve for T_2

$$T_2 = 625 - \sqrt{(625)^2 - 48400 - 2470W}$$

W = Watts of power flow

The power flow per ceramic is half the power per ring. $W = \frac{P_o}{2}$ where P_o = power dissipation per ring.

P_o	W	T_2
0	0	40
20	10	61
40	20	84
60	30	107.5

CALCULATION - REGION 2 (See Fig. 8)

To find temperature T_3 use the heat drop equation $-dT\,K(T) = \frac{W L_1}{A}$

$$\left.\begin{aligned} L_1 &= .160 \text{ inch} = .406 \text{ cm} \\ A &= at = (.072)(.125)(2.54)^2 = .0581 \text{ cm}^2 \end{aligned}\right\} \text{(See Fig. 8)}$$

$K(T) = 2.5 - 4 \times 10^{-3} T$ See Fig. 2

$$\int_{T_3}^{T_2} -(2.5 - 4 \times 10^{-3})\, T\, dT = 7W$$

$$2.5(T_3 - T_2) - 2 \times 10^{-3}(T_3^2 - T_2^2) = 7W$$

$$T_3 = 625 - \sqrt{625^2 - 1250 T_2 + T^2 - 3500W}$$

To solve for T_3 use the results of the region 1 calculation for T_2 in the above equation.

$$W = \frac{P_o}{2}$$ where P_o is the power per ring.

P_o	W	T_2	T_3
0	0	40	40
20	10	61	92
40	20	84	154
60	30	107.5	223

CALCULATION - REGION 3 (See Fig. 40)

Region 3 is one quarter of the copper ring of the circuit. Region 3 starts at the center of the support ceramic and ends at a point half way between the supporting ceramics. This will be the hot spot on the circuit assuming uniform power density on the ring. To find the temperature drop across Region 3 assume this region is a rectangular bar with length L_3 and a cross-sectional area of XY. See Fig. 40.

Power is dissipated uniformly over the region and all power flows to the ceramic support.

$$\text{Power density} = \frac{P_o}{\pi d}$$

P_o = average power per ring in watts

$$\text{Power flowing in ring} = \frac{P_o}{\pi d} L = W(L)$$

L = the distance from the hot spot on the ring

The temperature drop equation is as follows:

$$-dT = \frac{W(L)\, dL}{AK}$$

$$W(L) = \frac{P_o}{\pi d}$$

$$A = XY = .0232\ cm^2 \quad \text{(See Fig. 40)}$$

$$K = 3.88\ \frac{watt}{cm - {}^{o}C} \quad \text{for copper}$$

$$\Delta T = \frac{1}{AK} \int_{O}^{L_3} \frac{P_o}{\pi d}\ L\ dL$$

$$\Delta T = \frac{1}{AK}\ \frac{P_o}{\pi d}\ \frac{L_3^2}{2} = \frac{1}{AK}\ \frac{P_o}{\pi d}\ \frac{\pi^2 d^2}{32}$$

$$\Delta T = \frac{P_o}{8}\ \frac{\pi d}{4}\ \frac{1}{AK}$$

$$\Delta T = \frac{P_o}{8}\ \frac{1.755}{(.0232)\ (3.88)}$$

$$\Delta T = 2.44\ P_o$$

$$T_4 = T_3 + \Delta T$$

P_o	ΔT	T_3	T_4
0	0	40	40
20	48.8	92	140.8
40	97.6	154	251.6
60	146	223	369

Calculation of RF Power Dissipation Per Ring

Average rf output power — 1 kw

Loss of ring-bar circuit — less than 1 db/8"

Use 1 db/8" in calculation

2 rings per period of circuit

Period — .312 inch

1 db of power corresponds to 26 percent

Average rf power at end of circuit — $\frac{.26\ (1000)}{8} = \frac{260 \text{ watts}}{8 \text{ inches}}$

$\frac{260}{8} = 3.25$ watts/inch

Number of rings per inch — $\frac{2}{.312} = 6.4$

Power/ring — $\frac{32.5}{6.4} = 5.07$ watts/ring

Calculation of Power Dissipation on Circuit Due to Beam Interception on the Circuit

Average rf power	1 kw
Beam efficiency	30 percent
Average beam power	$\frac{1000}{.3}$ = 3300 watts

Assume 5 percent beam interception with no drive. The circuit dissipation due to 5 percent beam interception is .05 (3300) watts = 165 watts

Assume this power goes to all rings

6.4 rings/inch
8" of circuit

Total rings = (6.4) (8) = 51 rings

Power per ring = $\frac{165}{51}$ = 3.24 watts/ring

Under full rf drive one will have lower transmission due to rf defocusing. Assume the circuit can dissipate 60 watts/ring. The power that can be dissipated per ring due to rf defocusing is as follows:

$$60 - \left[5.07 \text{ watts due to rf}\right] - \left[3.24 \text{ watts due to no drive}\right] = 51.69 \text{ watts}$$

Assume the 51.69 watts per ring occurs over the last inch of the circuit. This is a good estimate because rf defocusing occurs 3 db below saturation and there is about 3 db of gain per inch on the circuit. There are 6.4 rings per inch so the circuit can dissipate (6.4) (51.69) watts due to rf defocusing

$$(6.4)\ (51.69) = 330 \text{ watts}$$

In terms of beam interception this is as follows:

$$\frac{3300}{3300 \text{ watts in the beam}} = 10 \text{ percent}$$

5 percent of the beam is intercepted with no drive
10 percent of the beam in intercepted due to rf defocusing

15 percent = total circuit interception

Transmission is 85 percent

Power per ring at the output end of the circuit is as follows:

51.69 watts due to rf defocusing
5.07 watts due to rf loss of the circuit
3.24 watts due to no drive defocusing

60.00 watts = total dissipation per ring

Hot spot temperature = 369°C

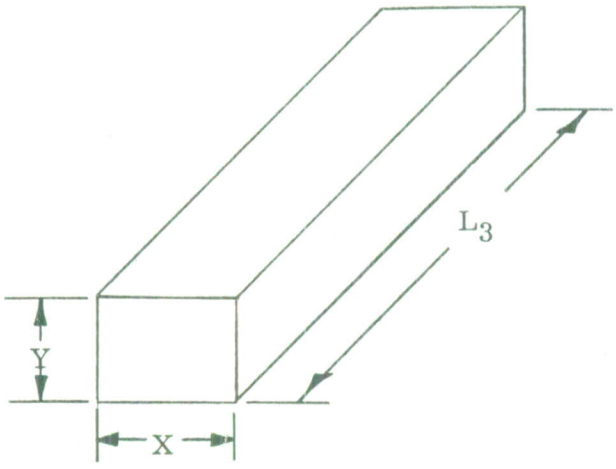

$L_3 = \frac{\pi d}{4} = \frac{\pi}{4}\left(\frac{O.D. + I.D.}{2}\right)$ ($\frac{1}{4}$ the circumference of ring)

$Y = \frac{O.D. - I.D.}{2}$ (thickness of ring)

X = .072 inch (width of ring)

O.D. = outside diameter of the ring = .93 inch

I.D. = inside diameter of the ring = .83 inch

$L_3 = \frac{(.88)(2.54)\pi}{4} = 1.755$ cm

Y = (050) (2.54) = .127 cm

X = (.072) (2.54) = .183 cm

Fig. 40 - Geometry used in the calculation of temperature drop across Region 3.

APPENDIX II

FINAL TEST DATA

The final packaged 100 kw L-band tube is shown in Fig. 41. This tube was packaged with a single reversal ceramic magnet stack with a diameter of 4 inches. The tube was tested at Watkins-Johnson Company on 27 February 1964. These tests were observed by Lincoln Cartledge and Marvin Siegel of the MIT Lincoln Laboratories. The data measured during these tests are shown in Figs. 42 and 43. Table III lists the operating parameters of the tube during these tests.

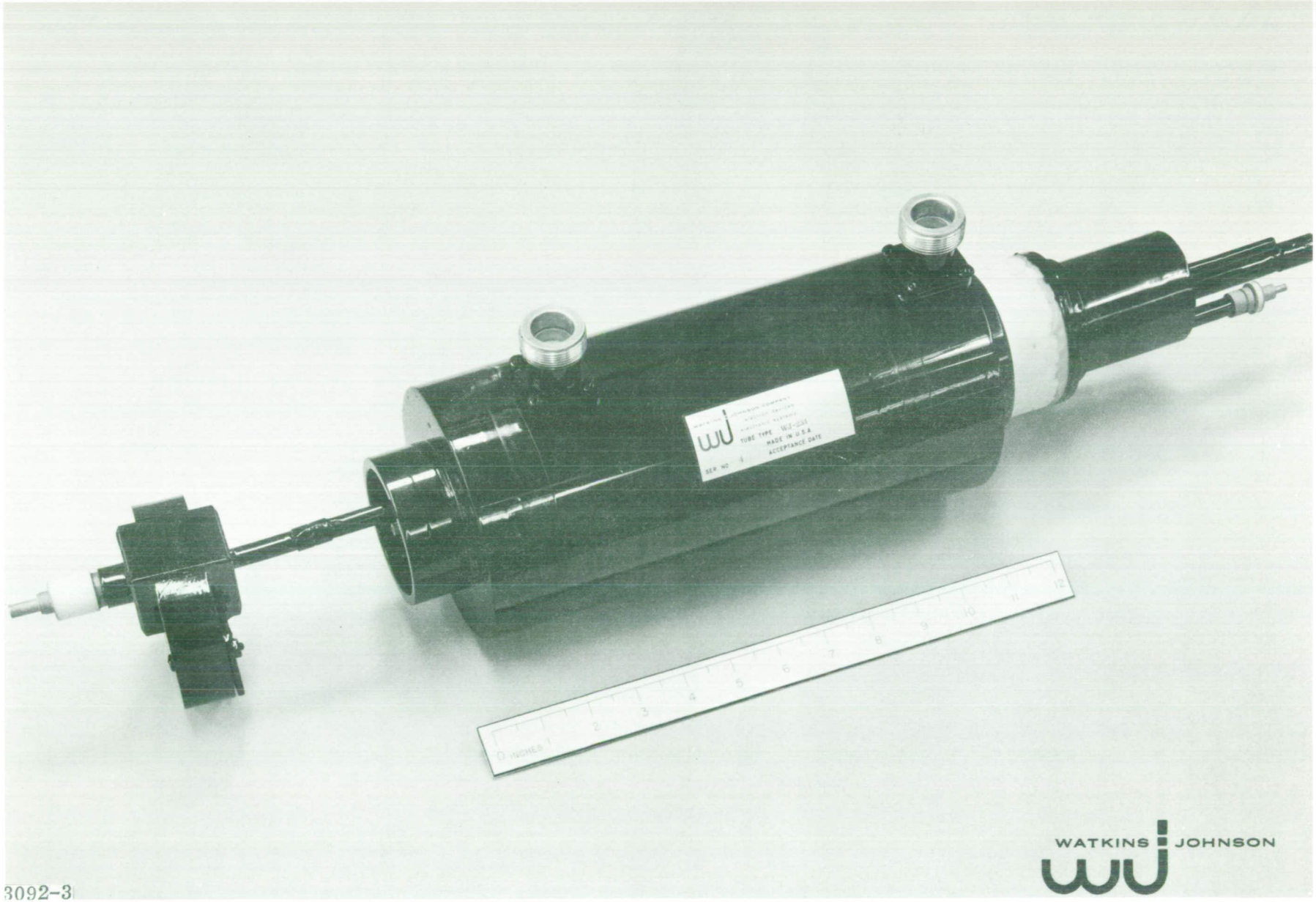

Fig. 41 - Photograph of the ceramic grounded cathode tube. The tube is focused by means of a single reversal ceramic magnet stack. Figs. 42 and 43 are plots of data measured on the ceramic barrel tube. Table III lists the operating parameter of the tube.

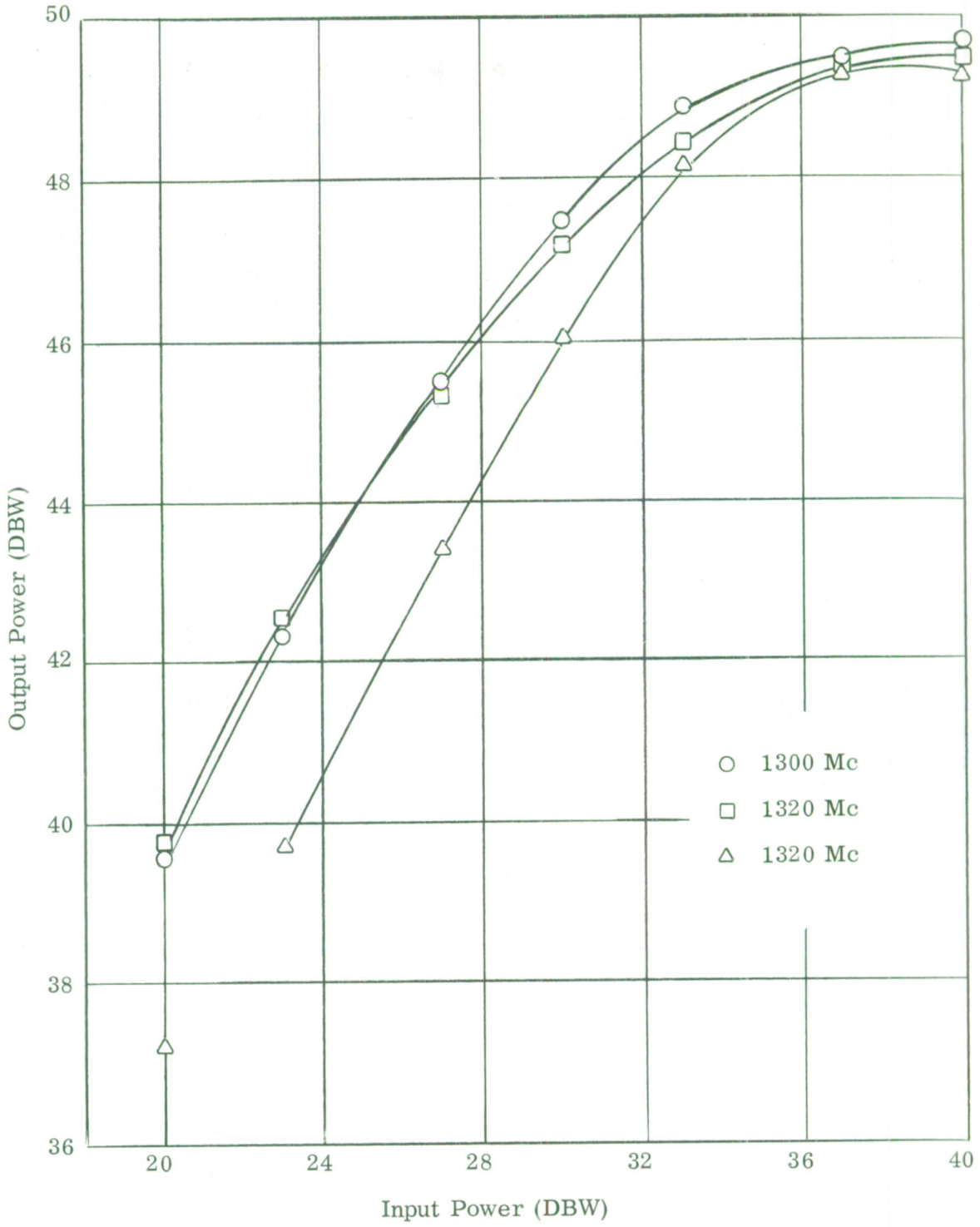

Fig. 42 - Output power vs input power as measured on the ceramic barrel grounded cathode tube shown in Fig. 41. Table III lists the operating parameters of the tube during these measurements.

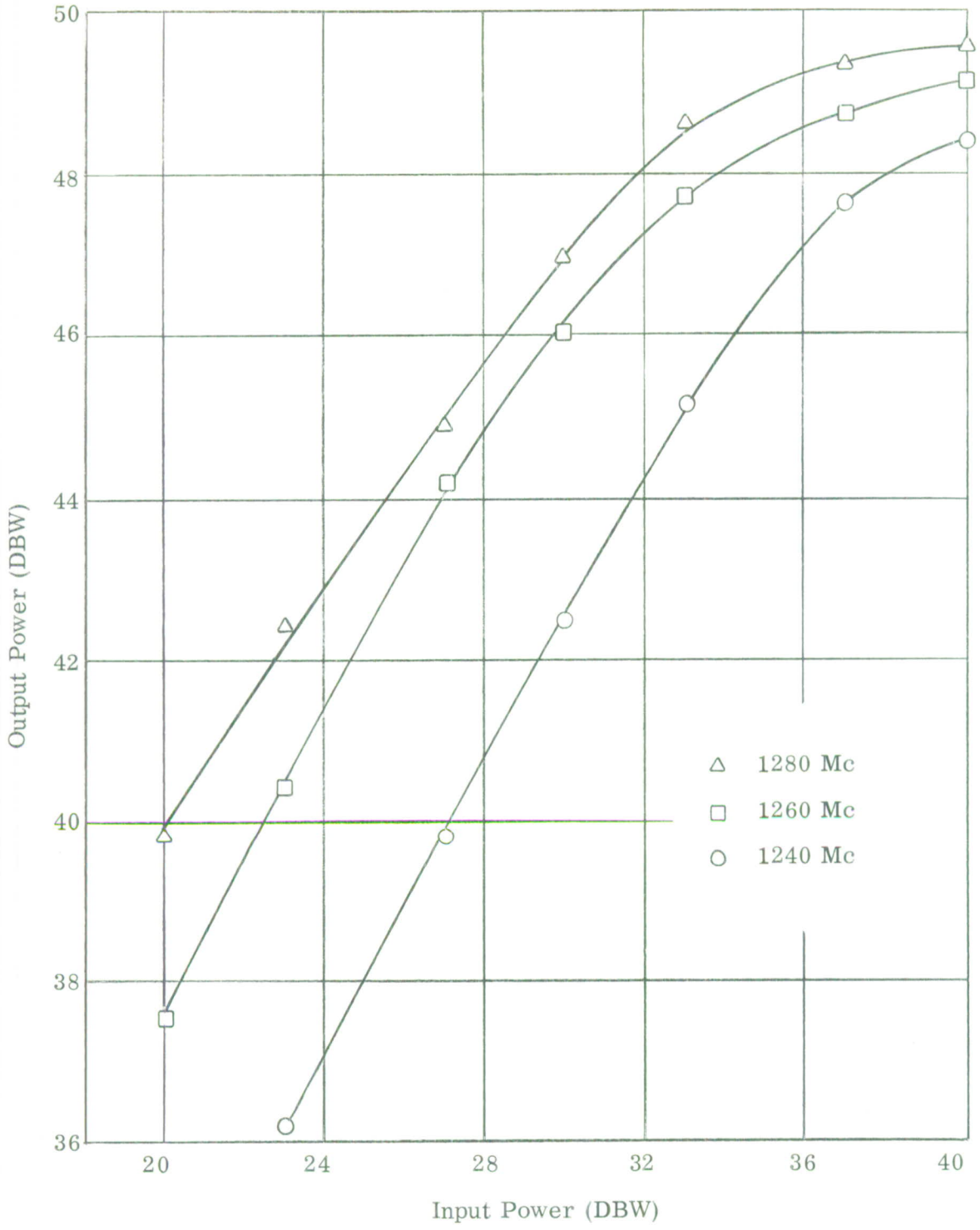

Fig. 43 - Output power vs input power as measured on the ceramic barrel grounded cathode tube shown in Fig. 41. Table III lists the operating parameters of the tube during these measurements.

TABLE III

Operating parameter of the grounded cathode tube shown in Fig. 41.

Beam voltage V_o	26.2 kv
Beam current I_o	17.25 amps
Collector current I_c	13.9 amps
Body current I_B	3.3 amps
Grid bias	-200 volts
Positive grid swing	200 volts
Grid current	5.4 amps
Heater voltage	14 volts
Heater voltage	5.2 volts
Heater power	73 watts